

A method for solving stochastic equations by reduced order models and local approximations

M. Grigoriu

Cornell University, Ithaca, NY 14853–3501, USA

ARTICLE INFO

Article history:

Received 20 September 2011

Received in revised form 8 March 2012

Accepted 11 June 2012

Available online 21 June 2012

Keywords:

Applied probability

Error estimation

Local approximations

Monte Carlo simulation

Random parameters

Stochastic equations

Stochastic reduced order models

Taylor expansion

Uncertainty quantification

ABSTRACT

A method is proposed for solving equations with random entries, referred to as stochastic equations (SEs). The method is based on two recent developments. The first approximates the response surface giving the solution of a stochastic equation as a function of its random parameters by a finite set of hyperplanes tangent to it at expansion points selected by geometrical arguments. The second approximates the vector of random parameters in the definition of a stochastic equation by a simple random vector, referred to as stochastic reduced order model (SROM), and uses it to construct a SROM for the solution of this equation.

The proposed method is a direct extension of these two methods. It uses SROMs to select expansion points, rather than selecting these points by geometrical considerations, and represents the solution by linear and/or higher order local approximations. The implementation and the performance of the method are illustrated by numerical examples involving random eigenvalue problems and stochastic algebraic/differential equations. The method is conceptually simple, non-intrusive, efficient relative to classical Monte Carlo simulation, accurate, and guaranteed to converge to the exact solution.

© 2012 Elsevier Inc. All rights reserved.

1. Introduction

Algebraic, differential, and other types of equations with random entries, referred to as stochastic equations (SEs), are used extensively in applied sciences and engineering to describe the behavior of physical systems. Stochastic equations can be viewed as mappings from their random entries to their solutions. For example, let U denote the displacement function of a beam with length $l > 0$ and random stiffness $K > 0$ that does not vary along the beam. Since U depends on a single real-valued random variable $Z = K$, the stochastic dimension of the problem is one. The random field $U(x, Z)$ satisfies the stochastic equation $ZU''(x, Z) = \alpha(x)$, $0 \leq x \leq l$, where the primes denote derivatives with respect to x and $\alpha(x)$ is a function describing the action on the beam that is assumed to be deterministic. Then $U(x, Z) = \beta(x)/Z$ with $\beta(x) = \int_0^x (\int_0^y \alpha(s) ds) dy$ for the boundary conditions $U(0, Z) = 0$ and $U'(0, Z) = 0$. Moments, distributions, and other properties of $U(x, Z)$ can be calculated simply from those of Z since the mapping $Z \mapsto U$ is known and has a simple form, for example, $E[U(x, Z)^r] = \beta^r E[1/Z^r]$ and $P(U(x, z) \leq u) = P(Z \geq \beta(x)/u)$ for $u > 0$. If stiffness varies randomly along the beam, that is, K becomes a real-valued random field $K(x) > 0$, the resulting problem has an infinite stochastic dimension since $\{K(x), 0 \leq x \leq l\}$ is an uncountable family of random variables. For calculations, $K(x)$ is usually approximated by a parametric random field $K_p(x, Z)$, that is, a deterministic function of x that depends on a finite-dimensional random vector Z , so that the solution $U(x, Z)$ is also a parametric random field. Although the mapping $Z \mapsto U$ is known, $U(x, Z) = \int_0^x (\int_0^y [\alpha(s)/K_p(x, Z)] ds) dy$, it is not possible to obtain simple formulas for moments, distribution, and other properties of U as for the case in which the beam stiffness is space-invariant.

E-mail address: mdg12@cornell.edu

Monte Carlo is the only general method for solving stochastic equations irrespective of their complexity. The method is asymptotically correct in the sense that its error vanishes as the sample size increases indefinitely. Statistics of the solution U of a SE are inferred from samples of this random element that are obtained by solving deterministic versions of this equation corresponding to samples of Z . The required sample size for a specified accuracy depends on the objective of the analysis, for example, first two moments, distributions, or other properties of U . Computational time, that can be significant when dealing with realistic problems, is the only limitation of the classical Monte Carlo method. The efficiency of the method can be improved significantly by a smart selection of samples of Z , for example, quasi Monte Carlo simulation [18,28], Latin hypercube sampling [22], and measure change [13, Section 5.4].

Stochastic Galerkin and collocation are perhaps the most popular approximate methods for solving stochastic equations, and have been applied to solve a broad range of problems that can be described by ordinary and partial differential equations with random entries [1–3,5,9,10,21,23–25,28]. The methods construct representations for the mapping $Z \mapsto U$ and use them to calculate properties of U . The initial versions of the stochastic Galerkin and collocation methods are practical for problems with relatively low stochastic dimensions, a restriction referred to as the curse of dimensionality. However, recent versions of these methods based on the Smolyak sparse grid collocation and other methods [26] have been applied successfully to solve problems with large stochastic dimensions. For example, the adaptive sparse grid collocation scheme proposed in [11] can be used to reduce the dimension of large stochastic problems by identifying the relevant coordinates of Z and biasing the samples toward these coordinates, the algorithms for selecting collocation points introduced in [27] can be used to solve problems with increasing stochastic dimension, the novel anisotropic Smolyak-based sparse grid collocation method in [20] has overcome the curse of dimensionality for a broad range of problems, the multi-element probabilistic collocation method in [9] has been applied to solve SEs with stochastic dimension up to 50 as well as nonlinear random vibration problems, and the ANOVA model in [28] provides solutions for complex stochastic incompressible and compressible flows problems that are much more efficient than those by Monte Carlo simulation.

The paper presents a novel non-intrusive method for solving stochastic equations that is viewed as an addition to the family of existing methods for this class of equations such as Monte Carlo simulation, stochastic Galerkin, and stochastic collocation. We assume that the random entries in the definition of a stochastic equation can be collected in an \mathbb{R}^d -valued random variable Z defined on a probability space (Ω, \mathcal{F}, P) and that the mapping $Z \mapsto U$ is measurable, so that U is a random function defined on the same probability space as Z . The random element U is completely defined by the mapping $Z \mapsto U$ and the probability law of Z , and can be a random vector, stochastic process, random field, or space–time random function depending on equation type. The proposed method for solving SEs combines features of (1) smart Monte Carlo simulation, in the sense that it uses a relatively small number of samples $\{\tilde{z}_k\}$ of Z to characterize this random vector in an optimal manner and (2) collocation method, in the sense that it interpolates between solutions $\{\tilde{u}_k\}$ of deterministic versions of stochastic equations obtained by replacing Z with $\{\tilde{z}_k\}$. The proposed method uses local interpolators, for example, hyperplanes tangent to the mapping $Z \mapsto U$ at $\{\tilde{u}_k\}$ to construct approximations for this mapping. We note that the samples $\{\tilde{z}_k\}$ of Z and corresponding deterministic solutions $\{\tilde{u}_k\}$ used in the proposed method can be used as interpolation points for collocation solutions.

Our approach is based on two recently developed methods for solving SEs. The first method constructs piecewise linear approximations for the solution U of a stochastic equation based on selected partitions $\{\Gamma_k\}$ of the range $\Gamma = Z(\Omega) \subset \mathbb{R}^d$ of Z and expansion points $\{\tilde{z}_k \in \Gamma_k\}$, $k = 1, \dots, m$, in these partitions [7,8]. The initial partition $\{\Gamma_k\}$ may be refined based on the information provided by deterministic solutions of the stochastic equation for $Z = \tilde{z}_k$, $k = 1, \dots, m$. The construction of the partition $\{\Gamma_k\}$, the selection of expansion points $\{\tilde{z}_k\}$, and the refinement of $\{\Gamma_k\}$ do not account for the probability law of Z . The second method approximates Z by a simple random vector \tilde{Z} with m samples $\{\tilde{z}_k\}$ of probabilities $\{p_k\}$ [14–16]. The vector \tilde{Z} , referred to as a stochastic reduced order model (SROM) for Z , has the same dimension as Z and its probability law is inferred from that of Z . Solutions $\{\tilde{u}_k\}$ of deterministic versions of a stochastic equation with $Z = \tilde{z}_k$, $k = 1, \dots, m$, are used to construct a SROM \tilde{U} for U , that is subsequently used to calculate properties of U approximately. The SROM \tilde{U} defines a piecewise constant approximation for the mapping $Z \mapsto U$.

The proposed method accounts for both the probability law of Z and properties of the mapping $Z \mapsto U$. SROMs for Z , rather than geometrical arguments, are used to select expansion points $\{\tilde{z}_k \in \Gamma\}$ and construct Voronoi partitions $\{\Gamma_k\}$ of Γ , so that the probability law of Z guides the selection of $\{\Gamma_k\}$ and $\{\tilde{z}_k\}$. Properties of mapping $Z \mapsto U$ at expansion points are used to construct first and higher order local approximations for the mapping $Z \mapsto U$, refine initial partitions $\{\Gamma_k\}$ via local SROMs, and construct superior approximations for $Z \mapsto U$. Bounds are developed to assess the accuracy of the proposed approximate solution and show that it converges to the exact solution as the partition $\{\Gamma_k\}$ of the parameter space Γ is refined. Numerical examples involving random eigenvalue problems, stochastic algebraic, and stochastic differential equations are presented to illustrate the implementation of the proposed method and quantify its accuracy. The method is conceptually simple, non-intrusive, efficient relative to classical Monte Carlo simulation, and guaranteed to converge to the exact solution as the Voronoi partition of the range of Z is refined.

2. Two methods for solving stochastic equations

Let U be the solution of a stochastic equation depending on an \mathbb{R}^d -valued random variable Z defined on a probability space (Ω, \mathcal{F}, P) . If the mapping $Z \mapsto U$ is measurable, then U is a random variable, stochastic process, random field, or time–space

random function depending on the type of its defining stochastic equation, that is also defined on (Ω, \mathcal{F}, P) . The probability law of U is induced by that of Z and the mapping $Z \mapsto U$.

Suppose U is a time–space, real-valued random function $U(t, x)$ defined on $I \times D$, where the time and space domains are bounded subsets of the real line and of an d' -dimensional space, that is, $I \subset \mathbb{R}$ and $D \subset \mathbb{R}^{d'}$. The marginal distribution and moment of order $q \geq 1$ of $U(t, x)$ are

$$P(U(t, x) \leq u) = E[1(U(t, x, \omega) \leq u)] = \int_{\Omega} 1(U(t, x, \omega) \leq u) P(d\omega) = \int_{\Gamma} 1(U(t, x, \xi) \leq u) dF(\xi) \quad \text{and} \quad (1)$$

$$E[U(t, x)^q] = E[U(t, x, \omega)^q] = \int_{\Omega} U(t, x, \omega)^q P(d\omega) = \int_{\Gamma} U(t, x, \xi)^q dF(\xi),$$

where $\Gamma = Z(\Omega) \subseteq \mathbb{R}^d$ is the range of Z and F denotes the distribution of Z . The integrals in Eq. 1 have the form $E[h(U(t, x))] = \int_{\Omega} h(U(t, x, \omega)) P(d\omega) = \int_{\Gamma} h(U(t, x, \xi)) dF(\xi)$, where $h: \mathbb{R} \rightarrow \mathbb{R}$ is a Borel measurable function. Similar integrals can be constructed for functionals of $U(t, x)$, for example, the distribution and moments of $\max_{t \in I, x \in D} \{U(t, x)\}$.

Let $\{A_k, k = 1, \dots, m\}$ be a measurable partition of Ω , so that the sets $\{\Gamma_k = Z(A_k)\}$ partition the range $\Gamma = Z(\Omega)$ of Z . Integrals $E[h(U(t, x))]$ as in Eq. 1 can be given in the form

$$E[h(U(t, x))] = \sum_{k=1}^m \int_{A_k} h(U(t, x, \omega)) P(d\omega) = \sum_{k=1}^m P(A_k) \left[\frac{1}{P(A_k)} \int_{A_k} h(U(t, x, \omega)) P(d\omega) \right] = E\{E[h(U(t, x)) | \mathcal{G}]\}, \quad (2)$$

where the σ -field $\mathcal{G} = \sigma(A_1, \dots, A_m)$ is generated by the partition $\{A_k\}$ of Ω and is coarser than \mathcal{F} . The expectation $E[h(U(t, x)) | \mathcal{G}](\omega) = \sum_{k=1}^m E[h(U(t, x)) | A_k] 1(\omega \in A_k)$ in Eq. 2 denotes the expectation of $h(U(t, x))$ conditional on \mathcal{G} , and

$$E[h(U(t, x)) | A_k] = \frac{1}{P(A_k)} \int_{A_k} h(U(t, x, \omega)) P(d\omega), \quad k = 1, \dots, m \quad (3)$$

are local averages of $h(U(t, x))$ over the subsets $\{A_k\}$ of Ω .

Generally, it is not possible to calculate exactly the expectation $E[h(U(t, x))]$ in Eqs. 2 and 3 since the probability law of U is not known. As previously mentioned, Monte Carlo simulation is the only general method for solving stochastic equations. The method delivers estimates for $E[h(U(t, x))]$ that are correct asymptotically as the sample size increases indefinitely. Let

$$\hat{V}[h(U(t, x))] = \frac{1}{n} \sum_{i=1}^n h(U^{(i)}(t, x)) \quad (4)$$

be an estimator for $E[h(U(t, x))]$, where $\{U^{(i)}(t, x)\}$ denote solutions of a stochastic equation corresponding to independent copies $\{Z^{(i)}\}$ of Z . The estimator is unbiased, that is, $E\{\hat{V}[h(U(t, x))]\} = E[h(U(t, x))]$, and converges to $E[h(U(t, x))]$ in probability as $n \rightarrow \infty$ since its variance is $\text{Var}\{\hat{V}[h(U(t, x))]\} = \text{Var}[h(U(t, x))]/n$, so that $P(|\hat{V}[h(U(t, x))] - E[h(U(t, x))]| > \varepsilon) \leq \text{Var}[h(U(t, x))]/(n\varepsilon^2)$ for an arbitrary $\varepsilon > 0$ by Chebyshev's inequality. This shows that Monte Carlo solutions converge to the correct result as the sample size increases indefinitely.

The following two sections summarize two methods that provide efficient approximations for $E[h(U(t, x))]$. Both methods construct partitions of the range $\Gamma = Z(\Omega)$ of Z and propose alternative representations for the local expectations in Eq. 3. The starting point of the first method is a partition of Γ that is constructed by geometrical considerations. The second method uses stochastic reduced order models (SROMs) for Z to partition Γ . We refer to these two distinct discretizations of Γ as geometrically-based and SROM-based partitions of the parameter space $\Gamma = Z(\Omega)$. For simplicity, we use a time-invariant stochastic equation $\mathcal{D}[U] = W$ to describe these two methods, where \mathcal{D} is a linear algebraic or differential operator that depends on Z while W does not depend on this random vector. If \mathcal{D} is a differential operator, boundary conditions need to be supplied for solution.

2.1. Geometrically-based partition

Let $\{\Gamma_k\}$ be a measurable partition of Γ and $\tilde{z}_k \in \Gamma_k$, $k = 1, \dots, m$, points in this partition. Geometrical arguments are solely used to select $\{\Gamma_k\}$ and $\{\tilde{z}_k\}$. For example, if Γ is a bounded rectangle in \mathbb{R}^d , $\{\Gamma_k\}$ can be rectangles with similar size and aspect ratio partitioning Γ and $\{\tilde{z}_k\}$ can be the centers of $\{\Gamma_k\}$ [7]. This selection is adequate if the coordinates of Z are independent random variables uniformly distributed in $[0, 1]$, so that $\Gamma = [0, 1]^d$ and F coincides with the Lebesgue measure in $[0, 1]^d$. However, partitions of identical geometry are likely to be inadequate if F differs from the Lebesgue measure. For this common case in applications, the shape and size of the subsets $\{\Gamma_k\}$ of Γ need to account for the probability law of Z .

Denote by $U(\tilde{z}_k)$ the solutions of the deterministic equations obtained from $\mathcal{D}[U] = W$ by setting $Z = \tilde{z}_k$, $k = 1, \dots, m$. The differentiation of $\mathcal{D}[U] = W$ with respect to a coordinate Z_r of Z gives $\partial \mathcal{D} / \partial Z_r [U] + \mathcal{D}[\partial U / \partial Z_r] = 0$, or $\mathcal{D}[\partial U / \partial Z_r] = -\partial \mathcal{D} / \partial Z_r [U]$, $r = 1, \dots, d$. The solutions of the latter equations with $Z = \tilde{z}_k$ gives the gradients $\nabla U(\tilde{z}_k)$ of $U(Z)$ at $Z = \tilde{z}_k$. Note that the same operator is used to calculate $U(\tilde{z}_k)$ and $\nabla U(\tilde{z}_k)$ at each expansion point \tilde{z}_k , $k = 1, \dots, m$. A method using generalized Green's function is used in [6] to calculate solutions $U(\tilde{z}_k)$ and $\nabla U(\tilde{z}_k)$ at $\{\tilde{z}_k\}$.

The solutions $U(\tilde{z}_k)$ and their gradients $\nabla U(\tilde{z}_k)$ can be used to construct the piecewise linear approximation

$$U_L(Z) = \sum_{k=1}^m [U(\tilde{z}_k) + \nabla U(\tilde{z}_k) \cdot (Z - \tilde{z}_k)] 1(Z \in \Gamma_k), \quad (5)$$

for $U(Z)$. The mapping $Z \mapsto U_L(Z)$ defined by Eq. 5 can be used to calculate approximately properties of $U(Z)$ by direct integration or Monte Carlo simulation.

Suppose as in Eq. 2 that our objective is to find the expectation of $h(U(Z))$, where $h: \mathbb{R} \rightarrow \mathbb{R}$ is a Borel measurable function. If h is also Lipschitz continuous, that is, there exists $c > 0$ such that $|h(\alpha) - h(\beta)| \leq c|\alpha - \beta|$, $\alpha, \beta \in \mathbb{R}$, the discrepancy between $h(U(Z))$ and $h(U_L(Z))$ can be measured by

$$E[|h(U(Z)) - h(U_L(Z))|] \leq cE[|U(Z) - U_L(Z)|] = cE\{E[|U(Z) - U_L(Z)||\mathcal{G}]\} = c \sum_{k=1}^m P(A_k) \left[\frac{1}{P(A_k)} \int_{\Gamma_k} |U(z) - U_L(z)| dF(z) \right], \quad (6)$$

where $\mathcal{G} = \sigma(A_1, \dots, A_m)$ and F denotes the distribution of Z . It has been suggested in [8] to use $c \sum_{k=1}^m P(A_k) \mathcal{E}_k$ as an approximation for $E[|h(U(Z)) - h(U_L(Z))|]$ in Eq. 6, where

$$\mathcal{E}_k = \frac{1}{P(A_k)} \int_{\Gamma_k} |\nabla U(\tilde{z}_k) \cdot (z - \tilde{z}_k)| dF(z) = \int_{\Gamma_k} |\nabla U(\tilde{z}_k) \cdot (z - \tilde{z}_k)| dF(z|\Gamma_k), \quad k = 1, \dots, m \quad (7)$$

are local errors involving the distribution $F(z|\Gamma_k) = P(Z \in (-\infty, z] \cap \Gamma_k) / P(Z \in \Gamma_k)$ of the conditional random variable $Z|Z \in \Gamma_k$ ([13, Section 2.17]).

For example, let $q \geq 0$ be an integer. The discrepancy between the moments of order $q+1$ of U and U_L can be evaluated from

$$\begin{aligned} |E[U^{q+1}] - E[U_L^{q+1}]| &= \left| E \left[(U - U_L) \sum_{r=0}^q U^{q-r} U_L^r \right] \right| \leq E \left[|U - U_L| \left| \sum_{r=0}^q U^{q-r} U_L^r \right| \right], \\ &\leq \alpha E[|U - U_L|] = \alpha \sum_{k=1}^m \int_{A_k} |U - U_L| dP, \\ &\simeq \alpha \sum_{k=1}^m \int_{A_k} |\nabla U(\tilde{z}_k) \cdot (Z - \tilde{z}_k)| dP \leq \alpha \sum_{k=1}^m \|\nabla U(\tilde{z}_k)\| \int_{A_k} \|Z - \tilde{z}_k\| dP \end{aligned} \quad (8)$$

provided $|\sum_{r=0}^q U^{q-r} U_L^r| \leq \alpha$ almost surely, where $\alpha > 0$ is a constant. Since the probability law of Z is known, the integrals $\int_{A_k} \|Z(\omega) - \tilde{z}_k\| P(d\omega)$ can be calculated.

Similar arguments can be used to assess the accuracy of the distribution of $U_L(Z)$. Since $F_U(u) = P(U(Z) \leq u) = E[1(U \leq u)] = \sum_{k=1}^m \int_{A_k} 1(U(Z(\omega)) \leq u) P(d\omega)$ and $F_{U_L}(u) = P(U_L(Z) \leq u) = E[1(U_L \leq u)] = \sum_{k=1}^m \int_{A_k} 1(U_L(Z(\omega)) \leq u) P(d\omega)$, we have

$$|F_U(u) - F_{U_L}(u)| \leq \sum_{k=1}^m \int_{A_k} |1(U(Z(\omega)) \leq u) - 1(U_L(Z(\omega)) \leq u)| P(d\omega), \quad (9)$$

where, as previously, $\{A_k\}$ is a measurable partition of Ω . Under the approximation $U - U_L \simeq \nabla U(\tilde{z}_k) \cdot (Z - \tilde{z}_k)$ on Γ_k , we have $|U - U_L| \leq \xi_k = \|\nabla U(\tilde{z}_k)\| \|Z - \tilde{z}_k\|$ by the Cauchy–Schwarz inequality, so that $U_L - \xi_k \leq U \leq U_L + \xi_k$ and the integrals $\int_{A_k} |1(U \leq u) - 1(U_L \leq u)| dP$ can be bounded approximately by $\int_{A_k} \max\{|1(U_L + \xi_k \leq u) - 1(U_L \leq u)|, |1(U_L - \xi_k \leq u) - 1(U_L \leq u)|\} dP$, and the latter integrals can be calculated.

An adaptive scheme has been used in [8] to identify members of the partition $\{\Gamma_k\}$ of Γ that need to be refined. The scheme is based on the relative magnitude of the local errors $\{\mathcal{E}_k\}$ in Eq. 7. A local error estimate \mathcal{E}_k is likely to contribute significantly to the global error if $U(Z)$ varies rapidly in Γ_k and/or the probability measure $P(Z \in \Gamma_k)$ is relatively large. If a local error \mathcal{E}_k is dominant, then Γ_k needs to be refined. This means that the set Γ_k is partitioned in measurable subsets $\{\Gamma_{k,i_k}\}$, $i_k = 1, \dots, m_k$, expansion points $\{\tilde{z}_{k,i_k}\}$ are selected in these subsets, and the original local approximation in Γ_k is replaced with a piecewise linear approximation of the type in Eq. 5 based on $\{\Gamma_{k,i_k}\}$ and $\{\tilde{z}_{k,i_k}\}$.

2.2. SROM-based partition

Suppose as in Eq. 5 that the solution $U(Z)$ is a real-valued random variable depending on a random vector Z . Let \tilde{Z} be a simple \mathbb{R}^d -valued random variable defined on the same probability space as Z with samples $\{\tilde{z}_k\}$ in $\Gamma = Z(\Omega)$ observed with probabilities $\{p_k \geq 0\}$, $k = 1, \dots, m$, such that $\sum_{k=1}^m p_k = 1$. Since \tilde{Z} is a random variable, $\{A_k = \tilde{Z}^{-1}(\tilde{z}_k)\}$ defines a measurable partition of Ω such that $P(A_k) = p_k$. The pairs $\{\tilde{z}_k, p_k\}$, $k = 1, \dots, m$, define completely the probability law of \tilde{Z} . We refer to \tilde{Z} as a stochastic reduced order model (SROM) for Z .

Properties of \tilde{Z} can be calculated simply. For example, the marginal distributions $\tilde{F}_i(\xi) = P(\tilde{Z}_i \leq \xi)$, marginal moments $\tilde{\mu}_i(q) = E[\tilde{Z}_i^q]$ of order $q \geq 1$, and correlations $\tilde{r}_{ij} = E[\tilde{Z}_i \tilde{Z}_j]$ of \tilde{Z} are

$$\tilde{F}_i(\xi) = \sum_{k=1}^m p_k 1(\tilde{z}_{k,i} \leq \xi), \quad \tilde{\mu}_i(q) = \sum_{k=1}^m p_k \tilde{z}_{k,i}^q, \quad \text{and} \quad \tilde{r}_{ij} = \sum_{k=1}^m p_k \tilde{z}_{k,i} \tilde{z}_{k,j}, \quad (10)$$

where $\{\tilde{z}_{k,i}\}$, $i = 1, \dots, d$, denote the coordinates of $\tilde{z}_k \in \mathbb{R}^d$ and $\xi \in \mathbb{R}$.

Our objective is to find a SROM \tilde{Z} for Z that is optimal in some sense. Optimality criteria using only the first two moments of Z have been used extensively to construct a class of SROMs called quantizers [12,19]. The objective function used to construct SROMs quantifies, in addition to the discrepancy between the first two moments of Z and \tilde{Z} , the discrepancy between higher order properties of these random vectors. For a selected model with size $m \geq 1$ and samples $\{\tilde{z}_k\}$, this function can have the form

$$e(p) = \sum_{s=1}^{\bar{s}} \beta_s e_s(p), \quad (11)$$

where $p = (p_1, \dots, p_m)$ denotes a probability vector, so that $p_k \geq 0$, $k = 1, \dots, m$, and $\sum_{k=1}^m p_k = 1$, $\{\beta_s > 0\}$ are weighting factors that can be used to emphasize various components of $e(p)$, and the functions $\{e_s(p)\}$ measures the discrepancy between various properties of Z and \tilde{Z} as a function of p . For example, we may set $\bar{s} = 3$, $e_1(p) = \sum_i \int (\tilde{F}_i(\xi) - F_i(\xi))^2 d\xi$, $e_2(p) = \sum_i \sum_{j=1}^q (\tilde{\mu}_i(\alpha) - \mu_i(\alpha))^2$, and $e_3(p) = \sum_{i,j} (\tilde{r}_{ij} - r_{ij})^2$, where $F_i(\xi) = P(Z_i \leq \xi)$, $\mu_i(\alpha) = E[Z_i^2]$, and $r_{ij} = E[Z_i Z_j]$.

Let $p = p^{(\text{opt})}$ be the probability vector minimizing the objective function $e(p)$ in Eq. 11 under the constraints $p_k \geq 0$, $k = 1, \dots, m$, and $\sum_{k=1}^m p_k = 1$ for an arbitrary set $\{\tilde{z}_k\}$, $k = 1, \dots, m$, of independent samples of Z , so that $e(p^{(\text{opt})})$ is the smallest value of the objective function for this set of samples. An optimal SROM \tilde{Z} for Z in the sense of the objective function in Eq. 11 can be obtained by calculating $p = p^{(\text{opt})}$ and $e(p^{(\text{opt})})$ for all sets of m independent samples of Z and retaining the set of m samples of Z with the smallest error $e(p^{(\text{opt})})$. Various optimization algorithms have been developed for constructing an optimal SROM \tilde{Z} for Z [14]. The construction of \tilde{Z} does not involve solutions of the defining stochastic equation for U .

Example 1. Let Z be a Gamma variable with density $f(z) = z^{\zeta-1} \eta^\zeta \exp(-\eta z) / \Gamma(\zeta)$, $z \geq 0$, and parameters $\zeta = 2$ and $\eta = 3$. The heavy dotted line in Fig. 1 shows the actual first 6 moments of Z . The approximate first 6 moments of Z delivered by a SROM \tilde{Z} of Z with $m = 20$ are in error by less than 1%, and are indistinguishable from the exact moments at the figure scale. In contrast, Monte Carlo estimates based on samples of size $m = 20$ of Z can be inaccurate. The thin lines in Fig. 1 are estimates of the first 6 moments of Z corresponding to 100 sets of independent samples of this random variable of length 20 each. Monte Carlo estimates of the first 6 moments of Z will match the accuracy of the corresponding moments of \tilde{Z} with $m = 20$ if based on approximately 50,000 independent samples of Z .

A SROM \tilde{Z} for Z induces a SROM \tilde{U} for U . The samples and probabilities of this models are $\{\tilde{u}_k = U(\tilde{z}_k)\}$ and $\{p_k\}$, $k = 1, \dots, m$. Similarly, SROMs can be defined for $h(U)$, where $h: \mathbb{R} \rightarrow \mathbb{R}$ is a Borel measurable function. Since $\tilde{Z}(\omega) = \sum_{k=1}^m \tilde{z}_k 1(\omega \in A_k)$, $\tilde{U}(\omega) = \sum_{k=1}^m \tilde{u}_k 1(\omega \in A_k)$, and $h(\tilde{U}(\omega)) = \sum_{k=1}^m h(\tilde{u}_k) 1(\omega \in A_k)$, formulas as in Eq. 10 can be applied to find properties of \tilde{U} and $h(\tilde{U})$, for example,

$$E[h(\tilde{U})] = \sum_{k=1}^m p_k h(\tilde{u}_k). \quad (12)$$

This expression also results from Eq. 2 with $h(U)$ replaced with the piecewise constant representation $h(\tilde{U}(\omega)) = \sum_{k=1}^m h(\tilde{u}_k) 1(\omega \in A_k)$ since $E[h(\tilde{U})] = \sum_{k=1}^m \int_{A_k} h(\tilde{U}) dP = \sum_{k=1}^m h(\tilde{u}_k) P(A_k)$. This observation also suggests that SROM-based approximations for $U(Z)$ are likely to be satisfactory if U varies slowly with Z in the subsets $\{\Gamma_k\}$ of Γ .

The implementation of a SROM-based method for solving stochastic equations requires to construct a SROM \tilde{Z} for Z , solve m deterministic versions of the stochastic equation defining U for $Z = \tilde{z}_k$, and find properties of \tilde{U} and functions of it. As previously stated, the last step involves elementary calculations.

In summary, the piecewise linear and piecewise constant approximations $U_L(Z)$ and $\tilde{U}(Z)$ for $U(Z)$ have the form

$$\begin{aligned} U_L(Z) &= \sum_{k=1}^m [U(\tilde{z}_k) + \nabla U(\tilde{z}_k) \cdot (Z - \tilde{z}_k)] 1(Z \in \Gamma_k) \quad \text{and} \\ \tilde{U}(Z) &= \sum_{k=1}^m U(\tilde{z}_k) 1(Z \in \Gamma_k), \end{aligned} \quad (13)$$

where $\{\Gamma_k\}$ is a measurable partition of the range Γ of Z and $\{\tilde{z}_k\}$ are points in $\{\Gamma_k\}$. For selected $\{\Gamma_k\}$ and $\{\tilde{z}_k\}$, $U_L(Z)$ provides a more accurate approximation for $U(Z)$ than $\tilde{U}(Z)$. However, $U_L(Z)$ and $\tilde{U}(Z)$ use distinct partitions $\{\Gamma_k\}$ of Γ and points $\{\tilde{z}_k\}$. The subsets $\{\Gamma_k\}$ and expansion points $\{\tilde{z}_k\}$ used to construct $U_L(Z)$ are selected by solely geometrical arguments. On the other hand, the selection of $\{\Gamma_k\}$ and $\{\tilde{z}_k\}$ for $\tilde{U}(Z)$ accounts explicitly for the probability law of Z via a SROM representation of this random vector.

3. A new method for solving stochastic equations

We have seen that the piecewise linear and piecewise constant approximations $U_L(Z)$ and $\tilde{U}(Z)$ for the solution $U(Z)$ of a stochastic equation have limitations. The construction of the piecewise linear approximation $U_L(Z)$ in Section 2.1 does not account for the probability law of Z . The piecewise constant approximation $\tilde{U}(Z)$ in Section 2.2 accounts for the probability

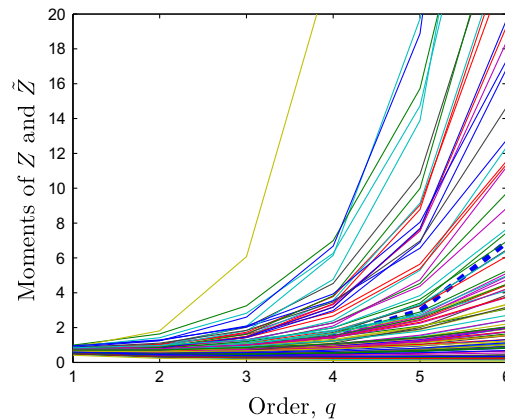


Fig. 1. Estimates of the first 6 moments of a Gamma random variable.

law of Z but approximates $U(Z)$ in a rather crude manner. A new method combining the desirable features of $U_L(Z)$ and $\tilde{U}(Z)$ is proposed. The method uses the samples $\{\tilde{z}_k\}$ of a SROM \tilde{Z} to construct a partition $\{\Gamma_k\}$ of the parameter space $\Gamma = Z(\Omega)$ and piecewise linear functions, rather than piecewise constant functions, to approximate the mapping $Z \mapsto U(Z)$.

Fig. 2 illustrates the construction of a partition $\{\Gamma_k\}$ for a parameter space Γ corresponding to a bivariate random variable Z with marginal beta distributions F_{Z_k} , $k = 1, 2$, of support $[1, 4]$ and shape parameters $p = 1$ and $q = 3$. The random vector Z is defined by the mappings $Z_k = F_{Z_k}^{-1} \circ \Phi(G_k)$, $k = 1, 2$, where $\{G_k\}$ are Gaussian variable with $E[G_k] = 0$, $E[G_k^2] = 1$, and $E[G_1 G_2] = 0.2$. The left panel in the figure shows the joint density of Z . The right panel shows contour lines of the density of Z . The symbols $*$ are the samples $\{\tilde{z}_k\}$ of a SROM \tilde{Z} of Z with $m = 20$. The sample of \tilde{Z} are far from equally spaced in $\Gamma = [1, 4]^2$. They are concentrated in the high probability subsets of Γ and explore the tails of the distribution of Z . The spider web in the figure is the Voronoi tessellation

$$\{\Gamma_k\} = \{z \in \Gamma : \|z - \tilde{z}_k\| \leq \|z - \tilde{z}_l\|, \quad l \neq k\}, \quad k, l = 1, \dots, m, \quad (14)$$

with nuclei or centers the samples $\{\tilde{z}_k\}$ of \tilde{Z} . The Voronoi tessellation provides an adequate partition for linear and higher order local approximations of mapping $Z \mapsto U(Z)$ since the accuracy of these approximations decreases with the distance from expansion points.

That the samples of \tilde{Z} have the properties in Fig. 2, that is, they are concentrated in subsets of high probability of Γ and explore the tails of the distribution of Z , results by construction. The components of the error $e(p)$ in Eq. 11 related to discrepancy between distributions and the first two moments of Z and \tilde{Z} can be made small if a sufficient number of samples of \tilde{Z} are located in the subset of Γ corresponding to likely values of Z , that is, the body of the distribution of this random vector. The components of $e(p)$ related to discrepancy between higher order moments of Z and \tilde{Z} can be made small if samples of \tilde{Z} are located in the subset of Γ corresponding to extreme values of Z , that is, the tails of the distribution of this random vector. The relative accuracy with which \tilde{Z} describes the body and the tails of the distribution of Z can be controlled by the weighting factors $\{\beta_s\}$ in Eq. 11 and/or by using alternative metrics for the errors $\{e_s(p)\}$ in this equation.

We have seen that the implementation of the piecewise linear approximation $U_L(Z)$ in Eq. 5 involves two steps. First, a partition $\{\Gamma_k\}$ of Γ and expansion points $\{\tilde{z}_k \in \Gamma_k\}$ are selected based on geometrical arguments. Second, the representation $U_L(Z)$ is constructed and used to calculate properties of $U(Z)$ approximately. The proposed method also involves two steps. First, a Voronoi partition $\{\Gamma_k\}$ of Γ is constructed, rather than being selected. The nuclei of the Voronoi partition $\{\Gamma_k\}$ are the samples $\{\tilde{z}_k\}$ of a SROM \tilde{Z} of Z . Second, the piecewise linear form in Eq. 5 corresponding to the samples $\{\tilde{z}_k\}$ of a SROM of Z and the associated Voronoi partition $\{\Gamma_k\}$ is constructed. The resulting representation of $U(Z)$ is denoted by $\tilde{U}_L(Z)$. The construction of Voronoi tessellation and the calculation of local averages of the type in Eq. 3 may not be feasible for high dimensional problems. However, it turns out that the cells $\{\Gamma_k\}$ do not have to be constructed explicitly and that local expectations can be estimated efficiently by Monte Carlo simulation.

Suppose the quantity of interest is an expectation $E[h(U)]$ of the type in Eq. 2, where $h: \mathbb{R} \rightarrow \mathbb{R}$ is a Borel measurable function. We approximate this function by $h(\tilde{U}_L)$ and estimate $E[h(\tilde{U}_L)]$ from n independent samples of Z . The integrals $\int_{\Gamma_k} h(\tilde{U}_L) dP$ in Eq. 3 with \tilde{U}_L in place of U can be estimated by $(1/n_k) \sum_{z_i \in \Gamma_k} h(\tilde{U}_L(z_i))$ so that $E[h(\tilde{U}_L(Z))] \simeq \sum_{k=1}^m (1/n_k) \sum_{z_i \in \Gamma_k} h(\tilde{U}_L(z_i))$, where n_k denotes the number of samples $\{z_i\}$ in Γ_k . A similar result can be obtained directly from the estimate $(1/n) \sum_{i=1}^n h(\tilde{U}_L(z_i))$ of $E[h(\tilde{U}_L)]$ written as

$$\begin{aligned} E[h(\tilde{U}_L(Z))] &\simeq \frac{1}{n} \sum_{i=1}^n h(\tilde{U}_L(z_i)) = \frac{1}{n} \sum_{k=1}^m \sum_{z_i \in \Gamma_k} h(\tilde{U}_L(z_i)) = \sum_{k=1}^m \frac{n_k}{n} \left[\frac{1}{n_k} \sum_{z_i \in \Gamma_k} h(\tilde{U}_L(z_i)) \right] \\ &= \sum_{k=1}^m \frac{n_k}{n} \left[\frac{1}{n_k/n} \left(\frac{1}{n} \sum_{z_i \in \Gamma_k} h(\tilde{U}_L(z_i)) \right) \right], \end{aligned} \quad (15)$$

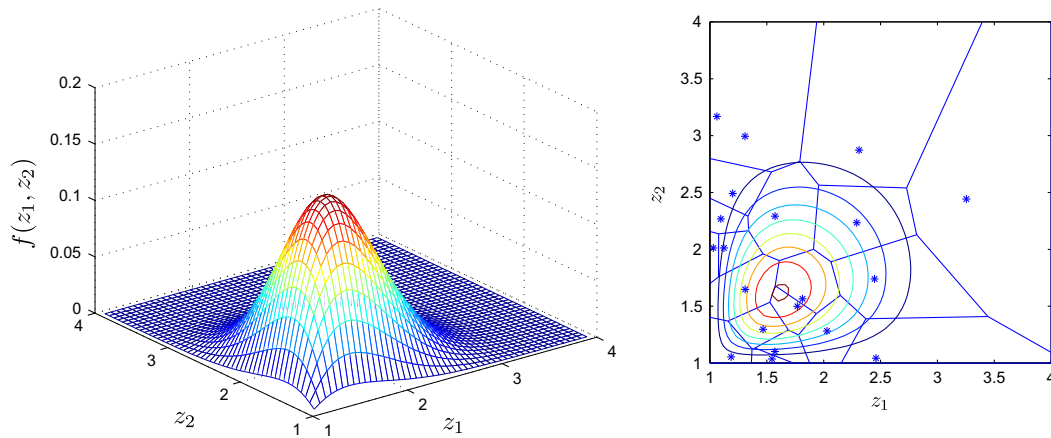


Fig. 2. Density of a bivariate Beta random variable Z (left panel), and contour lines of this density, sample $\{\tilde{z}_k\}$ of a SROM \tilde{Z} of Z with $m = 20$, and associated Voronoi partition $\{\Gamma_k\}$ of Γ (right panel).

so that $E[h(\tilde{U}_L(Z))]$ has the structure in Eqs. 2 and 3 since $n_k/n \rightarrow P(A_k)$ as $n \rightarrow \infty$ and the square bracket is an estimate for $\int_{A_k} h(\tilde{U}_L(Z)) dP/P(A_k)$. A simple algorithm has been used to select from a set of n independent samples $\{z_i\}$ of Z the subset that is closer to \tilde{z}_k than any other $\tilde{z}_l, l \neq k$, that is the samples of Z that belong to the cell Γ_k of the Voronoi tessellation of Γ centered on the sample $\{\tilde{z}_k\}$ of \tilde{Z} .

In summary, the approximations $\tilde{U}_L(Z)$ and $U_L(Z)$ have the same functional form, but use distinct partitions $\{\Gamma_k\}$ of Γ and expansion points $\{\tilde{z}_k\}$. Local errors of $\tilde{U}_L(Z)$ can be obtained from Eq. 7 with $\{\tilde{z}_k\}$ given by the samples of a SROM \tilde{Z} of Z , and can be estimated by

$$\hat{\mathcal{E}}_k = \frac{1}{n} \sum_{z_i \in \Gamma_k} \nabla U(\tilde{z}_k) \cdot (z_i - \tilde{z}_k) = \frac{1}{n/n_k} \left[\frac{1}{n_k} \sum_{z_i \in \Gamma_k} \nabla U(\tilde{z}_k) \cdot (z_i - \tilde{z}_k) \right], \quad (16)$$

where, as previously, $\{z_i\}$ are n independent samples of Z and $\{\Gamma_k\}$ are subsets of Γ centered on $\{\tilde{z}_k\}$.

Dominant estimates $\{\hat{\mathcal{E}}_k\}$ of local errors can be used to identify subsets that need to be refined, as proposed in [8]. If Γ_k is a subset that needs to be refined, samples of a local SROM for the conditional vector $Z|(Z \in \Gamma_k)$ can be used to refine the approximation $\tilde{U}_L(Z)$ in Γ_k by following the method proposed in this section. Samples of $Z|(Z \in \Gamma_k)$ can be used to estimate local averages of the type in Eq. 3 restricted to Γ_k .

Example 2. Let Z be a real-valued Beta random variable with range $\Gamma = Z(\Omega) = [a, b]$ and shape parameters $\{p, q\}$, so that $(Z - a)/(b - a)$ is a standard Beta variable with range $[0, 1]$, shape parameters $\{p, q\}$, and density $f(\xi) = \xi^{p-1}(1 - \xi)^{q-1}/B(p, q)$, where $\xi \in [0, 1]$ and $B(p, q)$ denotes the Beta function. Suppose the mapping $Z \mapsto U(Z)$ has the form $U(Z) = 1.25 - (Z - 0.5)^2$, so that $U'(Z) = -2(Z - 0.5)$ and $U''(Z) = -2$. Let $\tilde{z}_k \in [a, b]$, $k = 1, \dots, m$, be distinct points in $[a, b]$. The linear and quadratic approximations of the response surface $U(Z)$ corresponding to these expansion points are

$$\begin{aligned} U_L(Z) &= \sum_{k=1}^m [U(\tilde{z}_k) + U'(\tilde{z}_k)(Z - \tilde{z}_k)] 1(Z \in \Gamma_k) \quad \text{and} \\ U_Q(Z) &= \sum_{k=1}^m \left[U(\tilde{z}_k) + U'(\tilde{z}_k)(Z - \tilde{z}_k) + \frac{1}{2} U''(\tilde{z}_k)(Z - \tilde{z}_k)^2 \right] 1(Z \in \Gamma_k). \end{aligned} \quad (17)$$

The selection of the partition $\{\Gamma_k\}$ of $\Gamma = Z(\Omega)$ and of the expansion points $\{\tilde{z}_k\}$ differentiate the approximate representations $U_L(Z)$, $\tilde{U}(Z)$, and $\tilde{U}_L(Z)$.

The method in Section 2.1 partitions Γ in, for example, rectangles $\{\Gamma_k\}$ of the same size whose centers define the expansion points $\{\tilde{z}_k\}$. The rectangles $\{\Gamma_k\}$ are the intervals $\{\Gamma_k = [(k-1)\Delta z, k\Delta z]\}$, $k = 1, \dots, m$, in our case, where $\Delta z = (b - a)/m$. The linear approximation of $U(Z)$ in Eq. 17 can be used to calculate the expectation of $h(U(Z))$ approximately from

$$\begin{aligned} E[h(U_L(Z))] &= E\{E[h(U_L(Z))|\mathcal{G}]\} = E\left\{\sum_{k=1}^m 1_{A_k} \frac{1}{P(A_k)} \int_{A_k} h(U_L(Z)) dP\right\} \\ &= P(A_k) \left[\frac{1}{P(A_k)} \int_{A_k} h(U(\tilde{z}_k) + U'(\tilde{z}_k)(Z - \tilde{z}_k)) dP \right], \end{aligned} \quad (18)$$

where $h: \mathbb{R} \rightarrow \mathbb{R}$ is a Borel measurable function, $\{A_k = Z^{-1}(\Gamma_k)\}$ is a measurable partition of Ω , and the square brackets are local expectations of $h(U_L(Z))$ over $\{\Gamma_k\}$. Since the subsets $\{\Gamma_k\}$ of Γ are selected, the probabilities $\{P(A_k)\}$ and the local expectations of $h(U_L(Z))$ can be calculated analytically or numerically. The calculation of the probabilities and local expectations in Eq. 18 is simple for one-dimensional problems but can pose a notable computational challenge when dealing with high dimensional problems. The solid line in Fig. 3 is the distribution $F(u) = P(U(Z) \leq u)$ of $U(Z)$ for $a = 0.5$, $b = 4$, $p = 1/2$, and $q = 3$. The dotted line gives the distribution of $U_L(Z)$ for $m = 5$. The unfavorable performance of $U_L(Z)$ relates to the distribution of Z , that emphasizes arguments close to the left end of the range $[a, b]$ of this variable, the properties of the mapping $Z \mapsto U(Z)$, that is symmetric about $(a + b)/2$ and reaches its largest value at this point, and the selection of the partition $\{\Gamma_k\}$ and the expansion points $\{\tilde{z}_k\}$. The distribution of $U_L(Z)$ improves significantly as m increases.

The expansion points $\{\tilde{z}_k\}$ for the approximation $\tilde{U}_L(Z)$ are the samples of a SRM \tilde{Z} of Z with $m = 5$. We use a SRM \tilde{Z} whose samples $\{\tilde{z}_k\}$ and probabilities $\{p_k\}$ are $\{0.5239, 0.5840, 0.8788, 1.4604, 2.4068\}$ and $\{0.1630, 0.2896, 0.2487, 0.1633, 0.1353\}$, respectively. The solid heavy lines in Fig. 4 show the distribution $F(u)$ of $U(Z)$ for the same parameters as in Fig. 3. The thin solid lines are SRM-based approximations for $F(u)$. The heavy dotted lines in the left and right panels of the figure are approximations of the distribution of $U(Z)$ based on the linear and quadratic approximations in Eq. 17 corresponding to \tilde{Z} , that is, the approximations, $\tilde{U}_L(Z)$ and $\tilde{U}_Q(Z)$. These approximations are superior to the SRM-based approximation for $F(u)$. The quadratic form $\tilde{U}_Q(Z)$ provides a more accurate approximation for the distribution of $U(Z)$ than $\tilde{U}_L(Z)$. The approximation of $F(u)$ based on $\tilde{U}_Q(Z)$ is indistinguishable from $F(u)$ at the figure scale.

4. Error bounds

We have seen that the discrepancy between $U(Z)$ and its piecewise linear approximations $U_L(Z)$ and $\tilde{U}_L(Z)$ can be approximated by $\nabla U(\tilde{z}_k) \cdot (z - \tilde{z}_k)$ on Γ_k , where $\{\Gamma_k\}$, $k = 1, \dots, m$, denotes a measurable partition of the range Γ of Z . Since the distribution of Z is known and the partition $\{\Gamma_k\}$ of Γ and the expansion points $\{\tilde{z}_k\}$ are specified or constructed, properties of $\nabla U(\tilde{z}_k) \cdot (z - \tilde{z}_k)$ can be calculated and used to approximate statistics of the discrepancy between $U(Z)$ and $U_L(Z)$ or $\tilde{U}_L(Z)$. For example, $E[|U(Z) - \tilde{U}_L(Z)|]$ can be approximated by $\sum_{k=1}^m P(Z \in \Gamma_k) E[|\nabla U(\tilde{z}_k) \cdot (Z - \tilde{z}_k)| | Z \in \Gamma_k]$. This section develops bounds on the errors of piecewise linear and higher order approximations of $U(Z)$.

Properties of the remainder of Taylor expansions of $U(Z)$ are used to derive bounds on the discrepancy between $U(Z)$ and $U_L(Z)$ or $\tilde{U}_L(Z)$ and higher order approximations of the response surface $U(Z)$. It is assumed that $U(Z)$ is a real-valued random variable. We first consider the case in which Z has dimensions $d = 1$.

Theorem 1. If $d = 1$, $U(Z)$ has $q \geq 1$ continuous derivatives in Γ a.s., $U^{(q+1)}$ exists in Γ a.s., and Z has finite moments of order q , then

$$E[|U(Z) - \tilde{U}(Z)|] \leq \sum_{k=1}^m P(A_k) \frac{M_{q,k}}{(q+1)!} E[|Z - \tilde{z}_k|^{q+1} | A_k] \leq \frac{M_q}{(q+1)!} \sum_{k=1}^m P(A_k) E[|Z - \tilde{z}_k|^{q+1} | A_k] \quad (19)$$

where $0 < M_{q,k} < \infty$, $|U^{(q+1)}(z)| \leq M_{q,k}$ a.s., in Γ_k , and $M_q \geq M_{q,k}$ for $k = 1, \dots, m$.

Proof. The Taylor expansion of order q of $U(z)$ in Γ_k about \tilde{z}_k has the expression

$$U(z) = \sum_{r=0}^q \frac{U^{(r)}(c_k)}{r!} (z - \tilde{z}_k)^r + R_q(c_k, z) = \tilde{U}_q(z) + R_q(c, z),$$

where $R_q(c_k, z) = [U^{(q+1)}(c_k)/(q+1)!] (z - \tilde{z}_k)^{q+1}$ is the remainder and $c_k \in \Gamma_k$ ([4, Theorem 21.1]). We have

$$\begin{aligned} E[|U(Z) - \tilde{U}_q(Z)|] &= \sum_{k=1}^m P(A_k) E\left[\frac{U^{(q+1)}(c_k)}{(q+1)!} (Z - \tilde{z}_k)^{q+1} | A_k\right], \\ &\leq \sum_{k=1}^m P(A_k) \frac{M_{q,k}}{(q+1)!} E[|Z - \tilde{z}_k|^{q+1} | A_k], \\ &\leq \frac{M_q}{(q+1)!} \sum_{k=1}^m P(A_k) E[|Z - \tilde{z}_k|^{q+1} | A_k], \end{aligned}$$

by properties of the conditional expectations. The terms in the latter summation can be calculated from $P(A_k) E[|Z - \tilde{z}_k|^{q+1} | A_k] = \int_{\Gamma_k} |z - \tilde{z}_k|^{q+1} dF(z)$ by direct integration or Monte Carlo simulation, where F denotes the distribution of Z . \square

Example 3. The bound on $E[|U(Z) - \tilde{U}_q(Z)|]$ in Eq. 19 with $q = 1$ and $q = 2$ provides measures on the accuracy of the piecewise linear and quadratic approximations $\tilde{U}_L(Z) = \tilde{U}_1(Z)$ and $\tilde{U}_Q(Z) = \tilde{U}_2(Z)$. These bounds for the stochastic problem in Example 2 are

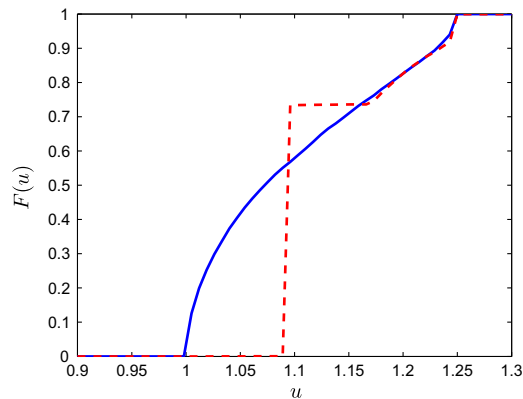


Fig. 3. Distributions of $U(Z)$ (solid line) and $U_L(Z)$ for $m = 5$ (dotted line) for $a = 0.5$, $b = 4$, $p = 1/2$, and $q = 3$.

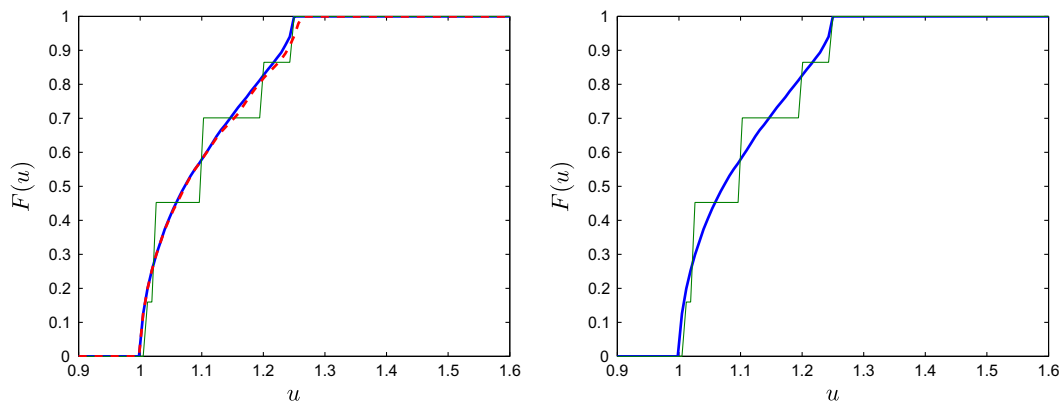


Fig. 4. Distribution $F(u)$ (solid heavy line), SROM-based approximation of $F(u)$ (solid thin line), and approximations of $F(u)$ by the proposed method with $m = 5$ based on $U_L(Z)$ (left panel) and $U_Q(Z)$ (right panel).

$$E\left[\left|U(Z) - \tilde{U}_L(Z)\right|\right] \leq \frac{M_1}{2!} \sum_{k=1}^m \int_{\Gamma_k} |z - \tilde{z}_k|^2 dF(z) \quad \text{and}$$

$$E\left[\left|U(Z) - \tilde{U}_Q(Z)\right|\right] \leq \frac{M_2}{3!} \sum_{k=1}^m \int_{\Gamma_k} |z - \tilde{z}_k|^3 dF(z),$$

where F denotes the distribution of Z , $M_1 = \max\{|a - 0.5|, |b - 0.5|\}$, and $M_2 = 2$. The discrepancy $E\left[\left|U(Z) - \tilde{U}_L(Z)\right|\right]$ is equal to 0.1478, 0.0348, 0.0142, and 0.0082 for $m = 5, 10, 15$, and 20. The corresponding bounds on $E\left[\left|U(Z) - \tilde{U}_L(Z)\right|\right]$ are 2.9190, 1.2208, 0.7430, and 0.5590. The discrepancy $E\left[\left|U(Z) - \tilde{U}_Q(Z)\right|\right]$ is zero for any $m \geq 1$ since the mapping $Z \mapsto U(Z)$ is quadratic. The bounds on $E\left[\left|U(Z) - \tilde{U}_Q(Z)\right|\right]$ are 0.1345, 0.0269, 0.0107, and 0.0060 for $m = 5, 10, 15$, and 20. For this problem, $\tilde{U}_Q(Z)$ provides a significant improvement over $\tilde{U}_L(Z)$.

Theorem 2. If $d > 1$, $U(Z)$ has continuous partial derivatives of order $q > 1$ in Γ a.s., the partial derivatives of order $q + 1$ exists in Γ a.s., and Z has finite moments of order q , then

$$E\left[\left|U(Z) - \tilde{U}_q(Z)\right|\right] \leq \frac{d}{q+d} \sum_{k=1}^m M_{q,k} P(A_k) E\left[\frac{\|Z - \tilde{z}_k\|^{q+d}}{\|Z - c_k\|^{d-1}} |A_k\right] \sum_{j=1}^{(q)} \prod_{i=1}^d \frac{1}{q_i!} \quad (20)$$

where $0 < M_{q,k} < \infty$ is such that $|\partial^{q+1} U(z) / (\partial z_1^{q_1} \dots \partial z_i^{q_i+1} \dots \partial z_d^{q_d})| \leq M_{q,k}$ for all $z \in \Gamma_k$, the summation $\sum_{q_1, \dots, q_d \geq 0; q_1 + \dots + q_d = q}$ is denoted by $\sum^{(q)}$, and c_k is a points on the open interval with ends \tilde{z}_k and z .

Proof. The multivariate Taylor formula at $z \in \mathbb{R}^d$ corresponding to expansion point \tilde{z}_k has the form

$$U(z) = \sum^{(\leq q)} \left(\prod_{j=1}^d \frac{(z_j - \tilde{z}_{kj})^{q_j}}{q_j!} \right) \frac{\partial^{q_1 + \dots + q_d} U(\tilde{z}_k)}{\partial z_1^{q_1} \dots \partial z_d^{q_d}} + R_q(c_k, z) = \tilde{U}_q(z) + R_q(c_k, z),$$

where $\sum^{(\leq q)} = \sum_{q_1, \dots, q_d \geq 0; q_1 + \dots + q_d \leq q}$, $\{z_j\}$ and $\{\tilde{z}_{kj}\}$ are the coordinates of z and \tilde{z}_k ,

$$\begin{aligned} R_q(c_k, z) &= \frac{\sum_{i=1}^d \alpha_i \|c_k - \tilde{z}_k\| \|z - \tilde{z}_k\|^n \left[\sum^{(q)} \left(\prod_{j=1}^d \frac{\alpha_j^{q_j}}{q_j!} \right) \frac{\partial^{q_1 + \dots + q_d} U(c_k)}{\partial z_1^{q_1} \dots \partial z_d^{q_d}} \right]}{\frac{1}{N(d)} \sum_{i=1}^d (q_i + 1) \frac{\|c_k - \tilde{z}_k\|}{\|z - \tilde{z}_k\|} \sum^{(q)} \left(\frac{\|z - c_k\|}{\|z - \tilde{z}_k\|} \right)^{q+d-1}} \\ &= \frac{\|z - \tilde{z}_k\|^{q+d}}{(q+d) \|z - c_k\|^{d-1}} \sum_{i=1}^d \alpha_i \sum^{(q)} \left(\prod_{j=1}^d \frac{\alpha_j^{q_j}}{q_j!} \right) \frac{\partial^{q_1 + \dots + q_d} U(c_k)}{\partial z_1^{q_1} \dots \partial z_d^{q_d}} \end{aligned}$$

denotes the remainder for the Taylor approximation of order q , $\{\alpha_j\}$ are the cosines of direction $z - \tilde{z}_k$, and $N(d)$ gives the number of terms in $\sum^{(q)}$. For $z \in \Gamma_k$, the remainder can be bounded by

$$|R_q(c_k, z)| \leq \frac{M_{q,k} d}{q+d} \frac{\|z - \tilde{z}_k\|^{q+d}}{\|z - c_k\|^{d-1}} \sum^{(q)} \prod_{j=1}^d \frac{1}{q_j!}$$

since $|\alpha_j| \leq 1$. This bound on the local error of the approximation \tilde{U}_q of order q of U and $E[U(Z) - \tilde{U}_q(Z)] = \sum_{k=1}^m P(A_k) E[R_q(c_k, Z) | A_k]$ yield Eq. 20.

For the special case $d = 1$, the bound in Eq. 20 takes the form

$$E[U(Z) - \tilde{U}_q(Z)] \leq \frac{1}{q+1} \sum_{k=1}^m M_{q,k} P(A_k) E[|Z - \tilde{z}_k|^{q+1} | A_k] \frac{1}{q!} \leq \frac{M_q}{(q+1)!} \sum_{k=1}^m P(A_k) E[|Z - \tilde{z}_k|^{q+1} | A_k],$$

with $M_q \geq M_{q,k}$, and coincides with the bound in Eq. 19. \square

Theorem 3. The discrepancy $E[U(Z) - \tilde{U}_q(Z)]$ can be made as small as desired by refining the partition $\{\Gamma_k\}$ of Γ .

Proof. Consider a sequence of partitions $\{\Gamma_k\}$ of Γ whose diameter decreases with m , that is, $\max_{1 \leq k \leq m, z', z'' \in \Gamma_k} \|z' - z''\| \sim O(\varepsilon_m)$, $\varepsilon_m > 0$, and $\varepsilon_m \rightarrow 0$ as $m \rightarrow \infty$. Since $P(A_k) E[\|Z - \tilde{z}_k\|^{q+d} / \|Z - c_k\|^{d-1} | A_k] \sim O(\varepsilon_m^{q+1})$, we have $E[U(Z) - \tilde{U}_q(Z)] \rightarrow 0$ as $m \rightarrow \infty$ by Eq. 20.

Similar results hold for functions $h(U)$ of U under some conditions, for example, functions $h: \mathbb{R} \rightarrow \mathbb{R}$ that are measurable and Lipschitz continuous. Results in this section also extend to vector-valued solutions U . \square

5. Applications

The implementation of the method for solving stochastic equations depending on a random vector Z involves two steps. First, a SRM \tilde{Z} with size m is developed for Z , and its samples $\{\tilde{z}_k\}$ are used to construct a Voronoi partition $\{\Gamma_k\}$ of the image Γ of Z . Second, a piecewise linear approximation \tilde{U}_L is developed based on $\{\tilde{z}_k\}$ and $\{\Gamma_k\}$, and used subsequently to calculate properties of U approximately.

We illustrate the implementation of the proposed method and assess its accuracy by examples involving solutions of random eigenvalue problems and stochastic algebraic and differential equations.

5.1. Random eigenvalue problem

Let A be an (n, n) real-valued symmetric matrix with random entries that are measurable functions of an \mathbb{R}^d -valued random variable Z defined on a probability space (Ω, \mathcal{F}, P) . It is assumed that A has distinct eigenvalues $\{\lambda_i(Z)\}$ and that $\det(A) \neq 0$ almost surely. As previously, let $\{\Gamma_k\}$, $k = 1, \dots, m$, be a measurable partition of the range $\Gamma = Z(\Omega)$ of Z and $\{\tilde{z}_k\}$ points in the members of this partition.

The corresponding piecewise linear approximations for the eigenvalues $\lambda_i(Z)$ of A follows from Eq. 5, and have the expressions

$$\lambda_{L,i}(Z) = \sum_{k=1}^m \left[\tilde{\lambda}_{i,k} + \sum_{r=1}^d \tilde{\lambda}_{i,k}^{(r)} (Z_r - \tilde{z}_{k,r}) \right] \mathbf{1}(Z \in \Gamma_k), \quad (21)$$

where $\tilde{\lambda}_{i,k} = \lambda_i(\tilde{z}_k)$,

$$\lambda_{i,k}^{(r)} = - \frac{c_{1,k}^{(r)} \lambda_{i,k}^{n-1} + \dots + c_{n-1,k}^{(r)} \lambda_{i,k} + c_{n,k}^{(r)}}{n \lambda_{i,k}^{n-1} + (n-1) c_{1,k} \lambda_{i,k}^{n-2} + \dots + c_{n-1,k}}, \quad k = 1, \dots, m, \quad (22)$$

$\{c_{i,k}\}$ are the coefficients $\{C_i\}$ of the characteristic equation $\det(A - \lambda I) = \lambda^n + C_1 \lambda^{n-1} + \dots + C_{n-1} \lambda + C_n = 0$ for $Z = \tilde{z}_k, c_{i,k}^{(r)} = \partial C_i(Z) / \partial Z_r$ at $Z = \tilde{z}_k$, $\{Z_r\}$ are the coordinates of Z , and $\{\tilde{z}_{k,r}\}$ denote the coordinates of \tilde{z}_k ([13, Section 8.3.2.3]). The expansion points $\{\tilde{z}_k\}$ can be the centers of a selected partition $\{\Gamma_k\}$ of Γ or the samples of a SROM model \tilde{Z} of Z . The representation in Eq. 21 can be used to find properties of the eigenvalues of A approximately. Similar approximations can be constructed for the eigenvectors of A [13, Section 8.3.2.3]).

Example 4. Let A be a random matrix depending on a real-valued random variable Z defined by $A = a + R$, where

$$a = \begin{bmatrix} 2.6 & -1.1 & 0.0 \\ -1.1 & 5.2 & -\sqrt{2} \\ 0.0 & -\sqrt{2} & 10 \end{bmatrix}, \quad R = Z \begin{bmatrix} 0.1 & -0.1 & 0.0 \\ -0.1 & 0.2 & 0.0 \\ 0.0 & 0.0 & 0.0 \end{bmatrix}, \quad \text{and}$$

$Z \sim U(-1, 1)$. The random coefficients of the characteristic polynomial $\det(A - \lambda I) = 0$ of A are $C_0 = 1$, $C_1 = -0.3Z - 17.8$, $C_2 = 0.01Z^2 + 3.82Z + 88.31$, and $C_3 = -0.1Z^2 - 8Z - 117.9$, so that $dC_0/dZ = 0$, $dC_1/dZ = -0.3$, $dC_2/dZ = 0.02Z + 3.82$, and $dC_3/dZ = -0.2Z - 8$. The gradients of $\lambda_i(Z)$ at $Z = \tilde{z}_k$ are

$$\lambda_{i,k}^{(1)} = -\frac{c_{1,k}^{(1)} \lambda_{i,k}^2 + c_{2,k}^{(1)} \lambda_{i,k} + c_{3,k}^{(1)}}{3\lambda_{i,k}^2 + 2c_{1,k} \lambda_{i,k} + c_{2,k}}, \quad k = 1, \dots, m,$$

with the previous notations.

Figs. 5 and 6 correspond to a partition of the range of Z in $m = 4$ equal intervals $\{\Gamma_k\}$ with centers $\{\tilde{z}_k = -1 + (k + 1/2)(2/m)\}$, $k = 1, \dots, m$. A SROM \tilde{Z} with parameters $\{\tilde{z}_k, p_k = 1/4\}$ is used for Z . For this model, the partitions of the range of Z in Sections 2.1 and 2.2 coincide. Values of these mappings at the expansion points $\{\tilde{z}_k\}$ are shown in Fig. 5.

Fig. 6 shows with heavy solid lines Monte Carlo estimates of the distributions $F_i(\lambda) = P(\lambda_i \leq \lambda)$, $i = 1, 2, 3$, of the eigenvalues of A . The estimates are based on $n = 1000$ independent samples of Z so that their construction requires to solve 1000 deterministic eigenvalue problems. The thin solid and heavy dotted lines are approximations of the distributions $F_i(\lambda)$ based on \tilde{Z} and piecewise linear approximations of the mappings $Z \mapsto \lambda_i(Z)$ based on \tilde{Z} , respectively. The latter approximation is a notable improvement over that based solely on \tilde{Z} . Since the gradients $\lambda_{i,k}^{(1)}$ in Eq. 22 are available analytically and $m = 4$, the construction of $\lambda_{L,i}(Z)$ in Eq. 21 involves solutions of only $m = 4$ deterministic eigenvalue problems.

Example 5. Consider the random matrix

$$A = \begin{bmatrix} Z_1 + Z_2 & -Z_2 & 0 \\ -Z_2 & Z_2 + Z_3 & -Z_3 \\ 0 & -Z_3 & Z_3 \end{bmatrix}, \quad (23)$$

where $Z_i = F^{-1} \circ \Phi(G_i)$, F is a Beta distribution with range $[a, b]$ and shape parameters $\{p, q\}$, $G_i \sim N(0, 1)$, $E[G_i G_j] = \rho^{|i-j|}$, $i, j = 1, 2, 3$, and $\rho \in (-1, 1)$. The coefficients of the characteristic equation for A are $C_1(Z) = -Z_1 - 2Z_2 - 2Z_3$, $C_2(Z) = Z_1 Z_2 + 2Z_1 Z_3 + 3Z_2 Z_3$, and $C_3(Z) = -Z_1 Z_2 Z_3$, so that $\partial C_1(Z) / \partial Z_r$ is $\{-1, -2, -2\}$, $\partial C_2(Z) / \partial Z_r$ is $\{Z_2 + 2Z_3, Z_1 + 3Z_3, 2Z_1 + 3Z_2\}$, and $\partial C_3(Z) / \partial Z_r$ is $\{-Z_2 Z_3, -Z_1 Z_3, -Z_1 Z_2\}$ for $r = 1, 2, 3$.

Let \tilde{Z} be a SROM for Z with parameters $\{\tilde{z}_k, p_k\}$, $k = 1, \dots, m$. The defining parameters for the corresponding SROMs of the eigenvalues $\{\lambda_i(Z)\}$ are $\{\tilde{\lambda}_{i,k} = \lambda_i(\tilde{z}_k), p_k\}$, $k = 1, \dots, m$. The formulas in Eqs. 21 and 22 with partitions $\{\Gamma_k\}$ and centers $\{\tilde{z}_k\}$ corresponding to \tilde{Z} provide piecewise linear approximations for the eigenvalues $\{\lambda_i(Z)\}$ of A .

The heavy solid lines in Figs. 7 and 8 are Monte Carlo estimates of the distributions $F_i(\lambda) = P(\lambda_i \leq \lambda)$, $i = 1, 2, 3$, of the eigenvalues of A based on 1000 independent samples of this matrix, so that their construction involves solutions of 1000 deterministic eigenvalue problems. The thin solid and heavy dotted lines are approximations of these distributions correspond to SROMs \tilde{Z} of Z and piecewise linear approximations based on these models. The left and right panels in the figures are for $m = 10$ and $m = 20$. The plots in Figs. 7 and 8 are for $\rho = 0.2$ and $\rho = 0.9$. The accuracy of the SROM- and SROM-based piecewise linear approximations of the distributions $F_i(\lambda)$ improves significantly as the size of \tilde{Z} increases from $m = 10$ to $m = 20$, in agreement with Theorem 3. Superior approximations result for $\rho = 0.9$ since a random vector with strongly correlated coordinates has less uncertainty in the sense that, given a coordinate of this vector, the uncertainty in its unspecified coordinates is reduced significantly. It can also be noted that approximations of $F_i(\lambda)$ based solely on \tilde{Z} are less satisfactory since SROMs \tilde{U} of U cannot provide any information on U outside the range $[\min_{1 \leq k \leq m} (U(\tilde{z}_k)), \max_{1 \leq k \leq m} (U(\tilde{z}_k))]$ of \tilde{U} .

Previous comments on the computational effort related to the implementation of the proposed method apply to this problem. The implementation of the piecewise linear approximations $\lambda_{L,i}(Z)$ in Eq. 21 involves solutions of $m = 10$ or $m = 20$ deterministic eigenvalue problems depending on the size of the SROM \tilde{Z} used to represent Z . As previously stated, the Monte Carlo estimates of the distributions $F_i(\lambda)$ are based on $n = 1000$ independent samples of Z , so that their construction involves solutions of 1000 deterministic eigenvalue problems.

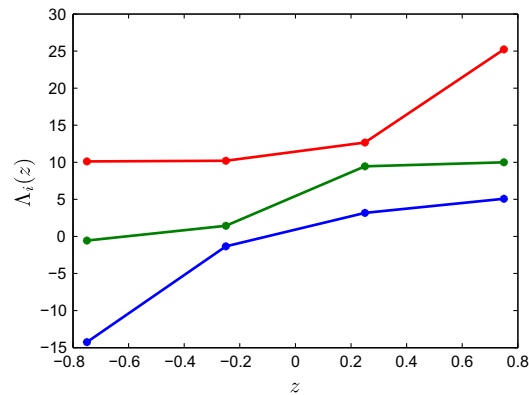


Fig. 5. Mappings $Z \mapsto \Lambda_i(Z)$, $i = 1, 2, 3$ at $Z = \tilde{z}_k$, $k = 1, \dots, 4$.

5.2. Stochastic algebraic equations

Suppose U satisfies a linear algebraic equation $AU = B$, where A is a random matrix whose entries are measurable functions on an \mathbb{R}^d -valued random variable Z and B may or may not be random. SROM-based piecewise linear approximations $\tilde{U}_L(Z)$ defined in a previous section can be used to approximate the response surface $U(Z)$ and calculate properties of the solution of $AU = B$.

Example 6. Let U be the solution of $AU = B$ with A in Eq. 23 and B the unit vector in \mathbb{R}^3 . We use the SROMs \tilde{Z} in Example 5 to construct $\tilde{U}_L(Z)$. Let $\{\tilde{z}_k, p_k\}$, $k = 1, \dots, m$, be the defining parameters of a SROM \tilde{Z} of Z , and denote by $U(\tilde{z}_k)$ the solution of the deterministic algebraic equation $AU = B$ for $Z = \tilde{z}_k$, $k = 1, \dots, m$. The gradients of $U(Z)$ at $Z = \tilde{z}_k$ satisfy the deterministic algebraic equations

$$A(Z) \frac{\partial U(Z)}{\partial Z_r} = -\frac{\partial A(Z)}{\partial Z_r} U(Z), \quad r = 1, 2, 3, \quad (24)$$

for $Z = \tilde{z}_k$, $k = 1, \dots, m$. Note that the deterministic algebraic equations for $U(\tilde{z}_k)$ and $\partial U(\tilde{z}_k)/\partial Z_r$, $r = 1, 2, 3$, have the same operator

$$A(\tilde{z}_k) = \begin{bmatrix} \tilde{z}_{k,1} + \tilde{z}_{k,2} & -\tilde{z}_{k,2} & 0 \\ -\tilde{z}_{k,2} & \tilde{z}_{k,2} + \tilde{z}_{k,3} & -\tilde{z}_{k,3} \\ 0 & -\tilde{z}_{k,3} & \tilde{z}_{k,3} \end{bmatrix} \quad (25)$$

for each $k = 1, \dots, m$. The partial derivatives $\{\partial U(Z)/\partial Z_r\}$ result simply from the definition of A , for example,

$$\frac{A(\tilde{z}_k)}{\partial Z_2} = \begin{bmatrix} 1 & -1 & 0 \\ -1 & 1 & 0 \\ 0 & 0 & 0 \end{bmatrix}.$$

The SROM-based piecewise linear approximation $\tilde{U}_L(Z)$ for $U(Z)$ is given by Eq. 13, and has the expression

$$\tilde{U}_L(Z) = \sum_{k=1}^m \left[U(\tilde{z}_k) - \sum_{r=1}^3 A(\tilde{z}_k)^{-1} \frac{\partial A(\tilde{z}_k)}{\partial Z_r} U(\tilde{z}_k) (Z_r - \tilde{z}_{k,r}) \right] 1(Z \in \Gamma_k). \quad (26)$$

Properties of $\tilde{U}_L(Z)$ can be calculated efficiently and accurately by, for example, Monte Carlo simulation, since its analytical form is available.

Fig. 9 shows estimates of the distributions $F_i(u) = P(U_i(Z) \leq u)$, $i = 1, 2, 3$, of the coordinates of $U(Z)$ obtained from 1000 independent samples of A (heavy solid lines), SROMs representations of Z (thin solid lines), and piecewise linear approximations $\tilde{U}_L(Z)$ of $U(Z)$ based on SROMs for Z (heavy dotted lines). The left and right panels are for $m = 10$ and $m = 20$. The accuracy of SROM-based solutions increases with m and ρ and SROM-based piecewise linear approximations are superior to those corresponding to SROMs, in agreement with previous numerical results. The SROM-based piecewise linear approximations in Fig. 10 for $m = 20$ are indistinguishable from $F_i(u)$ at the figure scale.

The Monte Carlo estimates of the distributions $F_i(u)$ in Figs. 9 and 10 are based on $n = 1000$ independent samples of A , so that their construction requires solutions of 1000 distinct deterministic algebraic equations. The construction of $\tilde{U}_L(Z)$ in Eq. 26 involves solutions of m distinct deterministic equations that need to be solved for $d + 1 = 4$ right sides. The total number

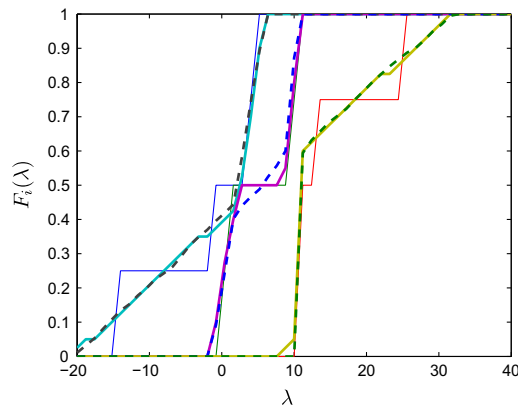


Fig. 6. Distributions $F_i(\lambda)$ (heavy solid lines) and approximations of these distributions by SROM (thin solid lines) and SROM-based piecewise linear approximations (heavy dotted lines).

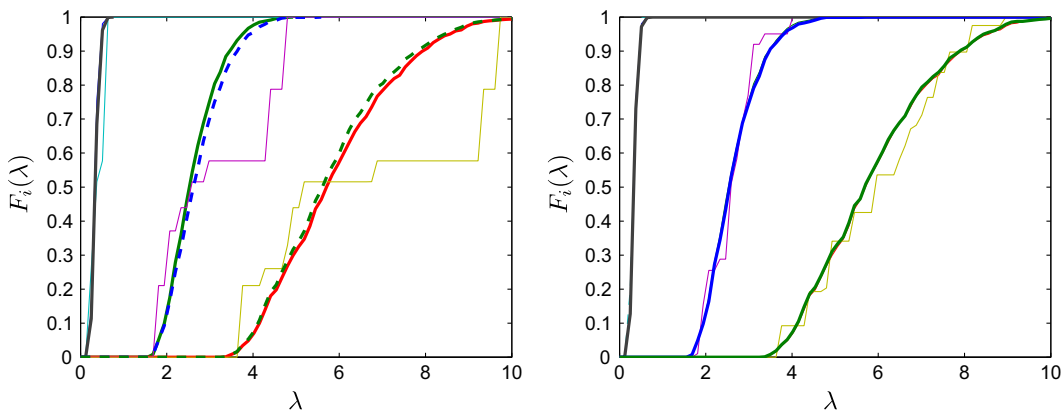


Fig. 7. Distributions $F_i(\lambda)$ (heavy solid lines) and approximations of these distributions by SROM (thin solid lines) and SROM-based piecewise linear approximations (heavy dotted lines) for $\rho = 0.2$, $m = 10$ (left panel), and $m = 20$ (right panel).

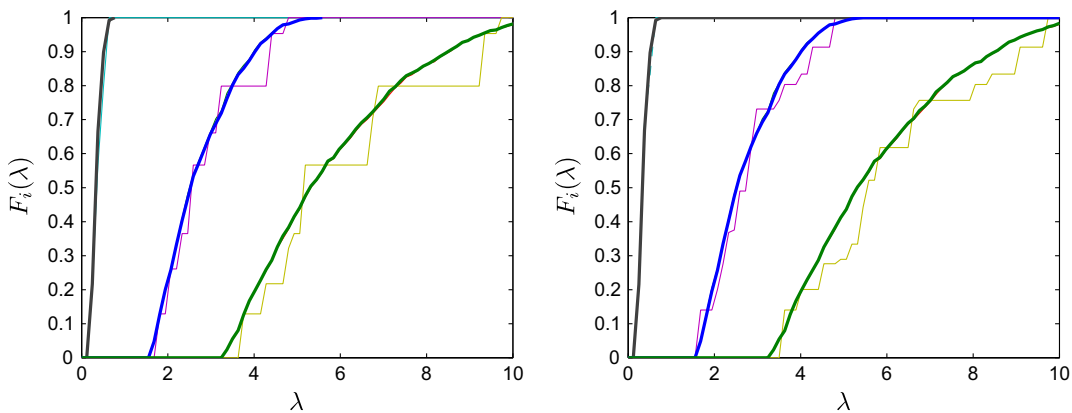


Fig. 8. Distributions $F_i(\lambda)$ (heavy solid lines) and approximations of these distributions by SROM (thin solid lines) and SROM-based piecewise linear approximations (heavy dotted lines) for $\rho = 0.9$, $m = 10$ (left panel), and $m = 20$ (right panel).

of deterministic solutions is $m(d + 1) = 4m$, that is, 40 solutions for $m = 10$ and 80 solutions for $m = 20$. The computation time associated with these solutions is much smaller than that corresponding to solving $m(d + 1)$ distinct deterministic algebraic equations since only m deterministic versions of A need to be inverted.

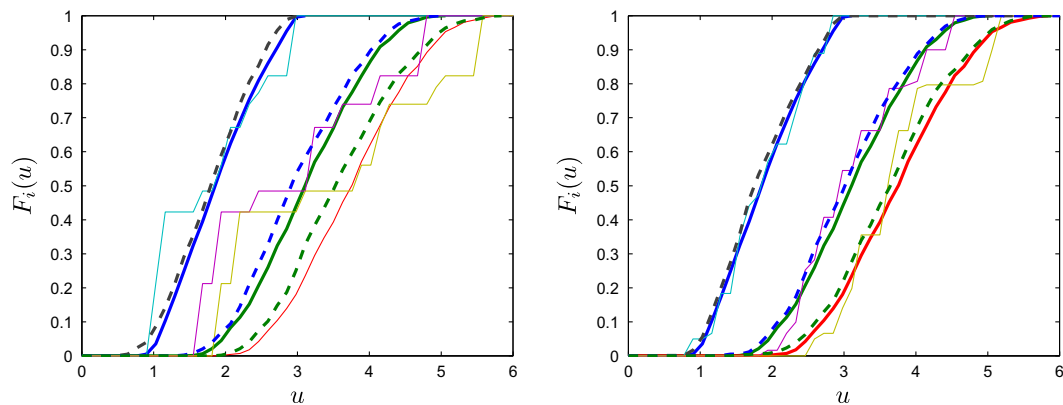


Fig. 9. Distributions $F_i(u)$ (heavy solid lines) and approximations of these distributions by SROM (thin solid lines) and SROM-based piecewise linear approximations (heavy dotted lines) for $\rho = 0.2$, $m = 10$ (left panel), and $m = 20$ (right panel).

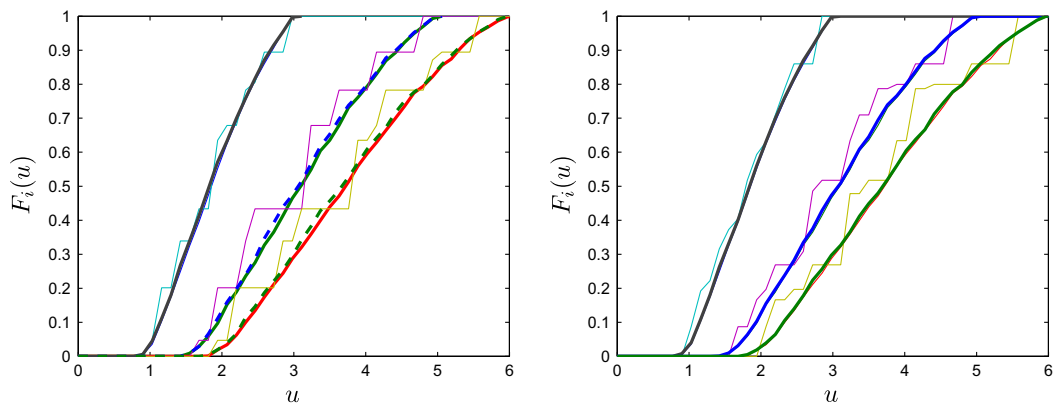


Fig. 10. Distributions $F_i(u)$ (heavy solid lines) and approximations of these distributions by SROM (thin solid lines) and SROM-based piecewise linear approximations (heavy dotted lines) for $\rho = 0.9$, $m = 10$ (left panel), and $m = 20$ (right panel).

5.3. Stochastic differential equations

Let $U(x, Z)$ be a real-valued random function that satisfies a differential equation with entries depending on a random vector Z , that is, a random function of the type considered in Section 2. As previously, we construct a SROM \tilde{Z} for Z and a piecewise linear approximation \tilde{U}_L for U , and use this approximation to estimate properties of U .

Example 7. Suppose U is the solution of the differential equation $d(A(x)U'(x))/dx = 0$, $x \in (0, 1)$, satisfying the boundary conditions $A(0)U'(0, Z) = -1$ and $U(1, Z) = 0$. It is assumed that $A(x, Z)$ is a parametric random function depending on an \mathbb{R}^d -valued random variable Z , that is,

$$A(x, Z) = \alpha_0 + \left(\sum_{r=1}^d Z_r \alpha_r(x) \right)^2, \quad (27)$$

where $\alpha_0 > 0$ is a constant and $\{\alpha_r\}$, $r = 1, \dots, d$, are deterministic functions. If $P(A(x, Z) > 0, 0 \leq x \leq 1) = 1$, then

$$U(x, Z) = \int_x^1 \frac{dy}{A(y, Z)} = \int_x^1 \frac{dy}{\alpha_0 + \left(\sum_{r=1}^d Z_r \alpha_r(y) \right)^2} \quad \text{a.s.}, \quad (28)$$

and the gradients of U with respect to the coordinates of Z can be obtained from

$$\frac{\partial U(x, Z)}{\partial Z_s} = -2 \int_x^1 \frac{\alpha_s(y) \left(\sum_{r=1}^d Z_r \alpha_r(y) \right) dy}{\left(\alpha_0 + \sum_{r=1}^d Z_r \alpha_r(y) \right)^2} \quad \text{a.s.}, \quad s = 1, \dots, d. \quad (29)$$

Numerical results are for the Beta random vector Z with $d = 3$ in Example 5 and its SROM \tilde{Z} in this example. The constant and the deterministic functions in Eq. 29 are $\alpha_0 = 0.2$ and $\alpha_r(x) = \sin(r\pi x)$, $r = 1, 2, 3$.

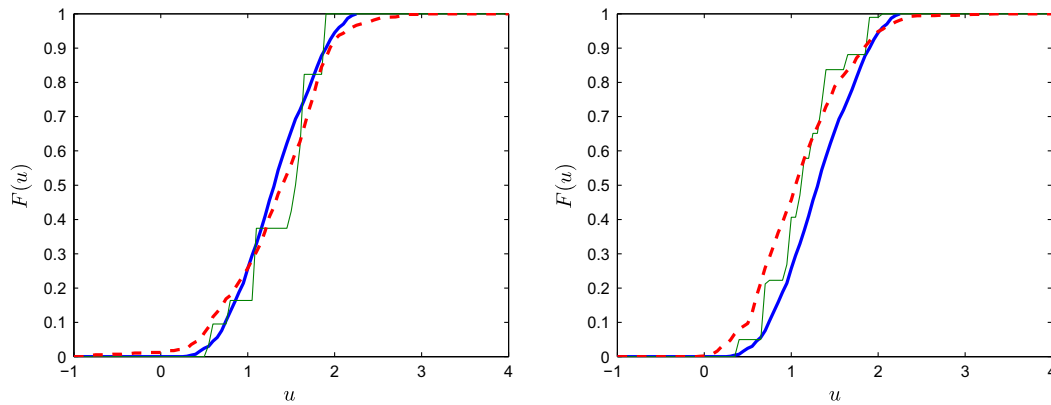


Fig. 11. Distribution $F(u)$ (heavy solid lines) and approximations of this distribution by SROM (thin solid lines) and SROM-based piecewise linear approximation (heavy dotted lines) for $\rho = 0.2$, $m = 10$ (left panel), and $m = 20$ (right panel).

Figs. 11 and 12 show with heavy solid lines Monte Carlo estimates of the distribution $F(u) = P(U(x, Z) \leq u)$ at $x = 0.2$ based on 1000 independent samples of $U(x, Z)$ for $\rho = 0.2$ and $\rho = 0.9$, respectively. The thin solid and heavy dotted lines are approximations of $F(u)$ based on \tilde{Z} and a piecewise linear approximation of $U(x, Z)$ based on \tilde{Z} . The left and right panels are for $m = 10$ and $m = 20$. The approximations of the distribution $F(u)$ have a similar behavior as that of the approximations in the previous examples. They improve with the model size m and correlation ρ and SROM-based piecewise linear approximations are superior to those based solely on SROMs.

The Monte Carlo estimates of $F(u)$ in Figs. 11 and 12 are based on $n = 1000$ independent samples of the random field $A(x, Z)$ so that their implementation requires solutions of 1000 deterministic versions of $d(A(x, Z)U'(x, Z))/dx = 0$. The implementation of the proposed method requires solutions of m and md deterministic versions of Eqs. 28 and 29, respectively, a total of $m(d + 1)$ solutions. These calculations can be reduced significantly if based on differential equations for the gradients of U as illustrated by the following example.

Example 8. Let $U(x)$ denote the temperature field in a rectangular specimen satisfying the stochastic partial differential equation

$$\nabla \cdot (A(x, \omega) \nabla U(x, \omega)) = 0, \quad (x, \omega) \in D \times \Omega, \quad (30)$$

with $D = (0, l_1) \times (0, l_2) \subset \mathbb{R}^2$, $U(0, x_2) = 0$ and $U(l_1, x_2) = 1$ for $x_2 \in (0, l_2)$, and $\partial U(x_1, 0)/\partial x_2 = \partial U(x_1, l_2)/\partial x_2 = 0$ for $x_1 \in (0, l_1)$. The conductivity $A(x)$ is the Beta translation random field

$$A(x) = \alpha + (\beta - \alpha) F_{\text{Beta}(p, q)}^{-1} \circ \Phi(G(x)) = h(G(x)), \quad x \in D, \quad (31)$$

where $F_{\text{Beta}(p, q)}$ denotes the distribution of a standard Beta random variable with range $[0, 1]$, shape parameters (p, q) , mean $p/(p + q)$, and variance $pq/[(p + q)^2(p + q + 1)]$, $0 < \alpha < \beta < \infty$ are constants, and $G(x)$ is a homogeneous Gaussian field with mean 0, variance 1, spectral density

$$s(v) = \frac{1}{2\pi\sqrt{1 - \rho^2}} \exp \left[-\frac{v_1^2 - 2\rho v_1 v_2 + v_2^2}{2(1 - \rho^2)} \right], \quad v = (v_1, v_2) \in \mathbb{R}^2 \quad (32)$$

and covariance function

$$c(\tau) = E[G(x)G(x + \tau)] = \exp \left[-\frac{\tau_1^2 + 2\rho\tau_1\tau_2 + \tau_2^2}{2} \right], \quad \tau = (\tau_1, \tau_2) \in \mathbb{R}^2, \quad (33)$$

with $\rho \in (-1, 1)$. Since the family of random variables $\{A(x), x \in D\}$ is uncountable, we represent the conductivity field by a linear model with dependent coefficient,

$$A_d(x, Z) = \sum_{i=1}^d Z_i \varphi_i(x), \quad x \in D, \quad (34)$$

where $\{\varphi_i(x)\}$ are specified deterministic functions and $Z = (Z_1, \dots, Z_d)$ is an d -dimensional random vector with dependent coordinates. We solve Eq. 30 with $A_d(x, Z)$ in place of $A(x)$, that is,

$$\nabla \cdot (A_d(x, Z(\omega)) \nabla U(x, Z(\omega))) = 0, \quad (x, \omega) \in D \times \Omega \quad (35)$$

and the same boundary conditions. The stochastic dimension of the problem in Eq. 35 is d . For simplicity, we call U the solution of this version of Eq. 30.

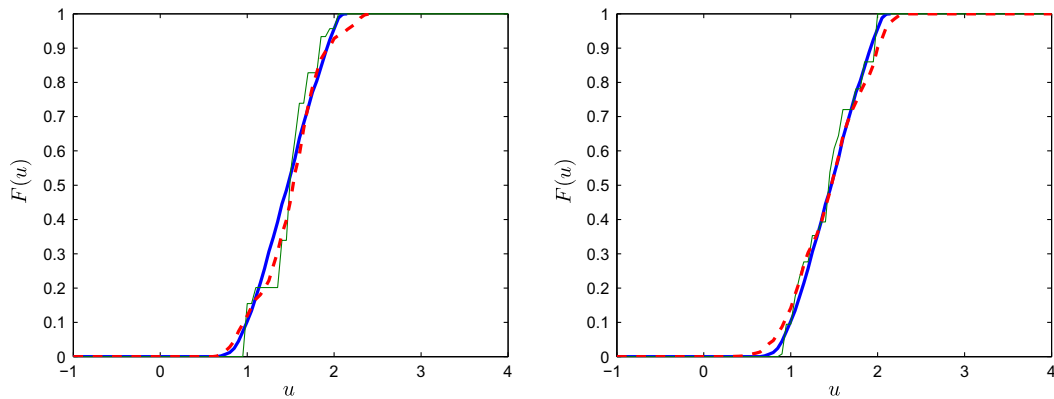


Fig. 12. Distribution $F(u)$ (heavy solid lines) and approximations of this distribution by SROM (thin solid lines) and SROM-based piecewise linear approximation (heavy dotted lines) for $\rho = 0.9$, $m = 10$ (left panel), and $m = 20$ (right panel).

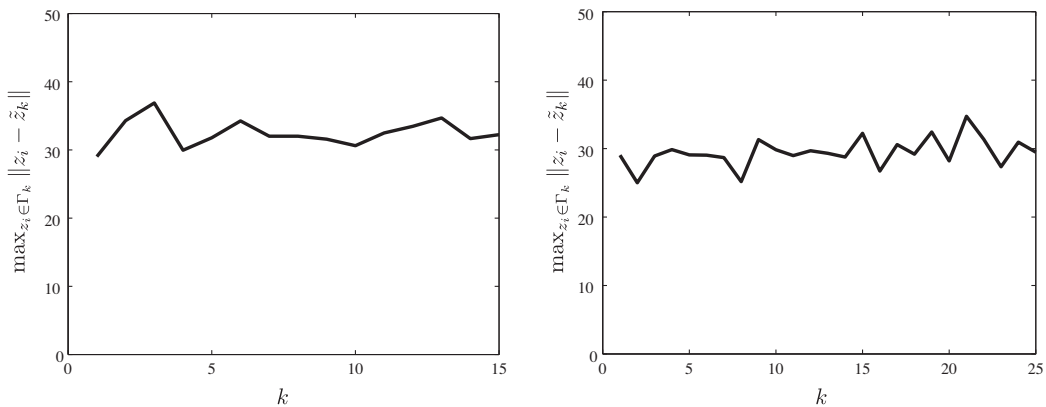


Fig. 13. An approximate measure for cell size corresponding to SROMs with $m = 15$ (left panel) and $m = 25$ (right panel).

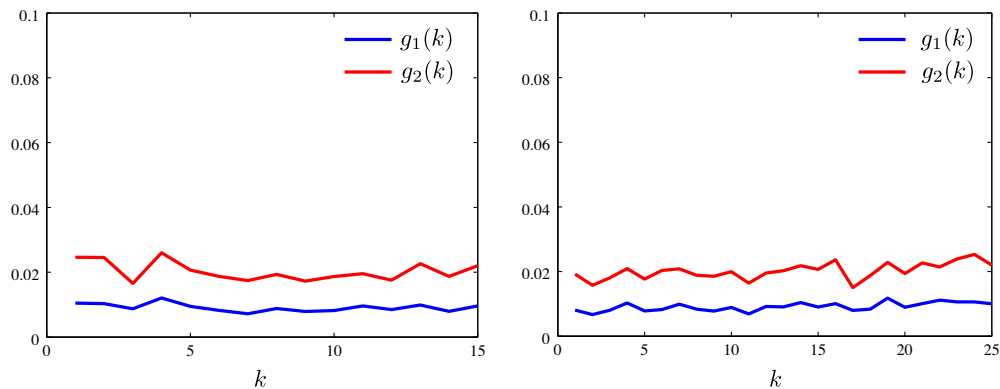


Fig. 14. Measures $g_1(k)$ and $g_2(k)$ of local gradients $\nabla \tilde{u}_x(x)$ for $m = 15$ (left panel) and $m = 25$ (right panel).

Numerical results are reported for $l_1 = 12$, $l_2 = 6$, $\alpha = 10$, $\beta = 100$, $p = 1$, $q = 3$, $\rho = 0.7$, and $d = 25$. This selection constitutes a severe test for the proposed method since the uncertainty in the conductivity field $A(x)$ is very high, for example, the coefficient of variation of $A(x)$ is 0.54. The functions $\{\varphi_i(x)\}$ in Eq. 34 are products of Chebyshev polynomials in x_1 and x_2 . Using an algorithm in [17], $n = 1000$ independent, equally likely samples $\{z_i\}$, $i = 1, \dots, n$, of Z have been obtained by minimizing the discrepancy between n independent samples of $A(x)$ and $A_d(x, Z)$. It is assumed that Z is completely described by the samples $\{z_i\}$, $i = 1, \dots, n$. This characterization of Z is used to construct SROMs \tilde{Z} for Z and Monte Carlo estimates for properties of U . The construction of Monte Carlo estimate requires $n = 1000$ solutions of distinct determination versions of Eq. 35 corresponding to $Z = z_i$, $i = 1, \dots, n$.

The construction of the piecewise linear representation \tilde{U}_L of U requires to find the deterministic functions $\{\tilde{u}_k\}$ and $\{\nabla \tilde{u}_k\}$, $k = 1, \dots, m$, that is, the functions U for m points $\{\tilde{z}_k\}$ in the range $\Gamma = Z(\Omega)$ of Z and the gradients of U with respect to the coordinates of Z at $\{\tilde{z}_k\}$. The expansion points for \tilde{U}_L are the samples $\{\tilde{z}_k\}$, $k = 1, \dots, m$, of a SROM \tilde{Z} for Z that are extracted from the set $\{z_i\}$, $i = 1, \dots, n$, by an optimization algorithm [14]. The functions $\{\tilde{u}_k\}$ are solutions of deterministic versions of Eq. 35 with $\{\tilde{z}_k\}$ in place of Z . The coordinates $V_r(x, Z) = \partial U(x, Z) / \partial Z_r$, $r = 1, \dots, d$, of the gradients of U at $\{\tilde{z}_k\}$ are obtained from the differential equations

$$\nabla \cdot (A_d(x, Z) \nabla V_r(x, Z)) = -\nabla \cdot \left(\frac{A_d(x, Z)}{\partial Z_r} \nabla U(x, Z) \right), \quad r = 1, \dots, d, \quad (36)$$

with $\{\tilde{z}_k\}$ in place of Z . The latter equation is derived from Eq. 35 by differentiating with respect to Z_r , $r = 1, \dots, d$. Since Eqs. 35 and 36 have the same differential operator, their solutions for $d + 1$ distinct right sides involves a single inversion of their common operator, that is, only m distinct deterministic operators need to be inverted. This observation increases significantly the efficiency of the finite element algorithm used for calculations. Since the mapping $Z \mapsto \tilde{U}_L$ is known and has a simple functional form, statistics of \tilde{U}_L can be obtained from samples of Z with a minimum computational effort. The Euclidean

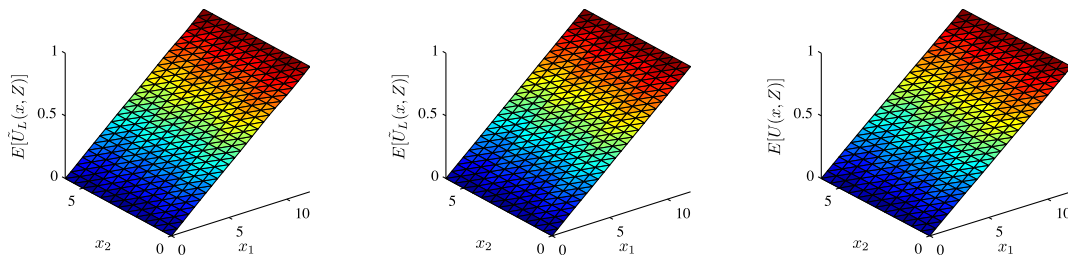


Fig. 15. Approximations of $E[U(x, Z)]$ based on a SROM with $m = 15$ (left panel), a SROM with $m = 25$ (middle panel), and Monte Carlo simulation (right panel).

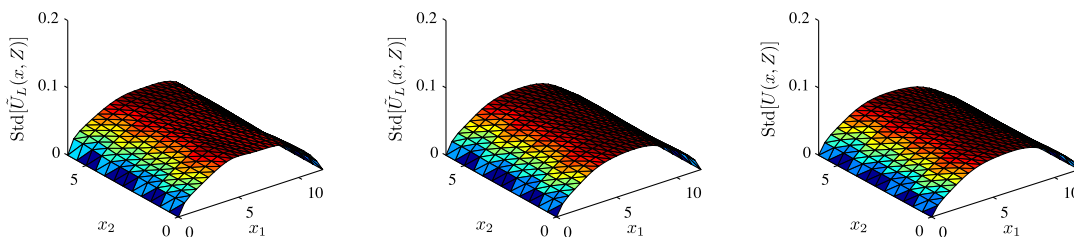


Fig. 16. Approximations of $\text{Std}[U(x, Z)]$ based on a SROM with $m = 15$ (left panel), a SROM with $m = 25$ (middle panel), and Monte Carlo simulation (right panel).

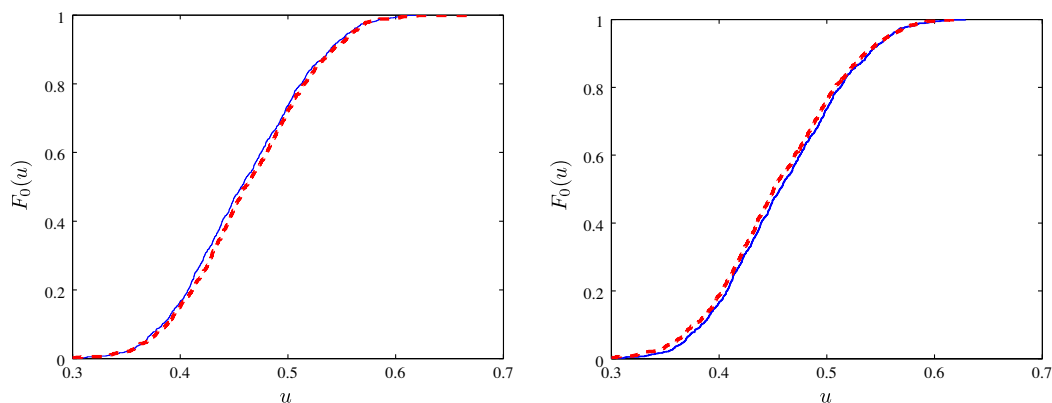


Fig. 17. A Monte Carlo estimate for $F_0(u) = P(U(x_0, Z) \leq u)$, $x_0 = (l_1/2, l_2/2)$, (think solid lines) and approximations of $F_0(u)$ based on SROMs with $m = 15$ (left panel) and $m = 25$ (right panel).

distance in \mathbb{R}^d is used to assign the samples $\{z_i\}$ of Z to the Voronoi cells $\{\Gamma_k\}$. For example, z_i is assigned to Γ_k if $\|z_i - \tilde{z}_k\| < \|z_i - \tilde{z}_l\|$ for all $l \neq k$. If $\|z_i - \tilde{z}_k\| = \|z_i - \tilde{z}_l\|$, z_i can be assigned to either \tilde{z}_k or \tilde{z}_l .

The approximate measure $\max_{z_i \in \Gamma_k} \|z_i - \tilde{z}_k\|$ for the size of the Voronoi cells is shown in the left and right panels of Fig. 13 for SROMs with $m = 15$ and $m = 25$, respectively. As expected, the cells for $m = 25$ are smaller on average than those for $m = 15$. Also, the cells $\{\Gamma_k\}$ for a given model size m have similar sizes. The magnitude of the gradients of $U(x, Z)$ at $\{\tilde{z}_k\}$ is quantify by

$$g_1(k) = \max_{1 \leq i \leq d} \max_{x \in D} |\partial \tilde{u}_k(x) / \partial z_i| \quad \text{and}$$

$$g_2(k) = \left((1/\text{vol}(D)) \int_D \|\nabla \tilde{u}_k(x)\|^2 dx \right)^{1/2}$$

and shown in Fig. 14 for $m = 15$ (left panel) and $m = 25$ (right panel). Since the cells $\{\Gamma_k\}$ have similar sizes and the gradients $\{\nabla \tilde{u}_k\}$ have similar magnitudes, we conclude that there is no need to refine the partition $\{\Gamma_k\}$ of I .

Fig. 15 shows approximations for $E[U(x, Z)]$ based a SROM with $m = 15$ (left panel), a SROM with $m = 25$ (middle panel), and Monte Carlo simulation (right panel). The Monte Carlo estimates are based on 1000 samples of $U(x, Z)$. Standard deviations of $U(x, Z)$ are in Fig. 16. The plots in the left, middle, and right panels are based on a SROM with $m = 15$, a SROM with $m = 25$, and Monte Carlo simulation using 1000 samples of $U(x, Z)$. The largest discrepancy between the means of $U(x, Z)$ by SROMs relative to Monte Carlo estimates are 0.012 for $m = 15$ and 5.5×10^{-3} for $m = 25$. Corresponding discrepancies for standard deviations are 0.095 for $m = 15$ and 4.8×10^{-3} for $m = 25$. The increase of the model size from $m = 15$ to $m = 25$ improves significantly the accuracy of the SROM-based approximations for $E[U(x, Z)]$ and $\text{Std}[U(x, Z)]$. A Monte Carlo estimate for the distribution $F_0(u) = P(U(x_0, Z) \leq u)$ of $U(x, Z)$ at $x_0 = (l_1/2, l_2/2)$ is shown with thin solid in Fig. 17. The heavy dotted lines in the figures are approximations of $F_0(u)$ based on SROMs with $m = 15$ (left panel) and $m = 25$ (right panel).

We conclude with comments on the computation time needed to implement Monte Carlo and proposed solutions for the stochastic equation in Eq. 35. A solution of a deterministic version of Eq. 35 using a finite element discretization with 325 nodes takes 0.0654 s on a laptop. The calculation of a solution \tilde{u}_k and all $d = 25$ coordinates of a gradient $\nabla \tilde{u}_k$ takes 1.2102 s. The time for calculating \tilde{u}_k and $\nabla \tilde{u}_k$ is less than $(d + 1) \times 0.0654 \simeq 1.7$ s since a single inversion of the deterministic operator corresponding to \tilde{z}_k needs to be performed to find \tilde{u}_k and $\nabla \tilde{u}_k$, as it can be seen from Eq. 36. The calculation of $n = 1000$ samples of U needed to construct Monte Carlo estimates takes $0.0654 \times 1000 \text{ samples} = 65.40$ s. The calculation of $\{\tilde{u}_k\}$ and $\{\nabla \tilde{u}_k\}$ for the proposed solution U_L based on a SROM with $m = 25$ takes $1.2102 \times m = 30.255$ s. The computation time for the Monte Carlo method is more than twice the time needed to implement the proposed method based on a SROM with size $m = 25$. This time is expected to be much larger than the computation time for the proposed method when dealing with large scale problems since the time for obtaining a single deterministic solution for this class of problems is much larger than that for solving a deterministic version of Eq. 35.

6. Conclusions

A method has been developed for finding properties of solutions of stochastic equations, that is based on two recently proposed methods for solving this class of equations. The first method constructs a piecewise linear approximation for the mapping $Z \mapsto U(Z)$ relating the solution U of a stochastic equation to its random entries Z , and uses it to characterize U . The expansion points used to construct local approximations and the supports of these approximations are selected by geometrical considerations. The second method constructs stochastic reduced order models \tilde{Z} for Z , calculates corresponding stochastic reduced order models \tilde{U} for U , and approximates properties of U by those of \tilde{U} . The representation \tilde{U} can be viewed as a piecewise constant approximation for the mapping $Z \mapsto U(Z)$ with expansion points given by the samples of \tilde{Z} .

The proposed method for solving stochastic equations constructs piecewise linear and higher order approximations for the mapping $Z \mapsto U(Z)$, that are similar to those used in the first method. However, it uses expansion points given by stochastic reduced order models \tilde{Z} for Z of the type considered in the second method. Voronoi tessellations centered on the samples of \tilde{Z} are employed to partition the range of Z . As a result, both the probability law of Z and properties of the exact mapping $Z \mapsto U(Z)$ are used to construct approximate representations for $U(Z)$. The proposed method is conceptually simple, non-intrusive, efficient relative to classical Monte Carlo simulation, accurate, and guaranteed to converge to the exact solution as the Voronoi partition of the range of Z is refined. The implementation of the method and its accuracy are illustrated by numerical examples involving random eigenvalue problems and stochastic algebraic and differential equations.

Acknowledgements

The work reported in this paper has been supported by the National Science Foundation under Grant CMMI-0969150. This support is gratefully acknowledged.

References

- [1] I.M. Babuška, K-M. Liu, On solving stochastic initial-value differential equations, *Mathematical Models and Methods in Applied Sciences* 13 (5) (2003) 715–745.

- [2] I.M. Babuška, F. Nobile, R. Tempone, A stochastic collocation method for elliptic partial differential equations with random input data, *SIAM Journal of Numerical Analysis* 45 (3) (2007) 1005–1034.
- [3] I.M. Babuška, R. Tempone, E. Zouraris, Galerkin finite element approximations of stochastic elliptic partial differential equations, *SIAM Journal of Numerical Analysis* 42 (2) (2004) 800–825.
- [4] R.L. Brabenec, *Introduction to Real Analysis*, PWS-KENT Publishing Company, Boston, 1990.
- [5] H.C. Elman, O.G. Ernst, D.P. O’Leary, M. Stewart, Efficient iterative algorithms for stochastic finite element method with applications to acoustic scattering, *Computer Methods in Applied Mechanics and Engineering* 194 (2005) 1037–1055.
- [6] D. Estep, M. Holst, M. Larson, Generalized Green’s functions and the effective domain of influence, *SIAM Journal of Scientific Computation* 26 (4) (2005) 1314–1339.
- [7] D. Estep, D. Neckels, Fast and reliable methods for determining the evolution of uncertain parameters in differential equations, *Journal of Computational Physics* 213 (2006) 530–556.
- [8] D. Estep, D. Neckels, Fast methods for determining the evolution of uncertain parameters in reaction-diffusion equations, *Computer Methods in Applied Mechanics and Engineering* 196 (2007) 3967–3979.
- [9] J. Foo, X. Wan, E. Karniadakis, The multi-element probabilistic collocation method (ME-PCM): Error analysis and applications, *Journal of Computational Physics* 227 (2008) 9572–9595.
- [10] P. Frauenfelder, C. Schwab, R.A. Todor, Finite element for elliptic problems with stochastic coefficients, *Computer Methods in Applied Mechanics and Engineering* 194 (2005) 205–228.
- [11] B. Ganapathysubramanian, N. Zabaras, Sparse grid collocation schemes for stochastic natural convection problems, *Journal of Computational Physics* 225 (2007) 652–685.
- [12] S. Graf, H. Luschgy, *Foundations of Quantization for Probability Distributions*, Springer, Lecture Notes in Mathematics (2000).
- [13] M. Grigoriu, *Stochastic Calculus: Applications in Science and Engineering*, Birkhäuser, Boston, 2002.
- [14] M. Grigoriu, Reduced order models for random functions. applications to stochastic problems, *Applied Mathematical Modelling* 33 (1) (2009) 161–175.
- [15] M. Grigoriu, Effective conductivity by stochastic reduced order models (SROMs), *Computational Materials Science* 50 (2010) 138–146, <http://dx.doi.org/10.1016/j.commatsci.2010.07.017>.
- [16] M. Grigoriu, Linear random vibration by stochastic reduced order models, *International Journal for Numerical Methods in Engineering* 82 (2010) 1537–1559, <http://dx.doi.org/10.1002/nme.2809>.
- [17] M. Grigoriu, Probabilistic models for stochastic elliptic partial differential equations, *Journal of Computational Physics* 229 (2010) 8406–8429, <http://dx.doi.org/10.1016/j.jcp.2010.07.023>.
- [18] L. Kocis, W.J. Whiten, Computational investigation of low-discrepancy sequences, *ASM Transactions on Mathematical Software* 23 (1997) 266–294.
- [19] Y. Linde, A. Buzo, R.M. Gray, An algorithm for vector quantizer design, *IEEE Transactions on Communications COM* 28 (1) (1980) 84–95.
- [20] F. Nobile, R. Tempone, C.G. Webster, An anisotropic sparse grid stochastic collocation method for partial differential equations with random input data, *SIAM Journal of Numerical Analysis* 46 (5) (2008) 2411–2442.
- [21] C. Schwab, R.A. Todor, Karhunen–Loève approximation of random fields by generalized fast multipole methods, *Journal of Computational Physics* 217 (2006) 100–122.
- [22] M. Stein, Large sample properties of simulation using Latin hypercube sampling, *Technometrics* 29 (1987) 143–151.
- [23] X. Wan, G.E. Karniadakis, An adaptive multi-element generalized Polynomial Chaos methods for stochastic differential equations, *Journal of Computational Physics* 209 (2) (2005) 617–642, <http://dx.doi.org/10.1016/j.jcp.2005.03.023>.
- [24] X. Wan, G.E. Karniadakis, Multi-element generalized polynomial chaos for arbitrary probability measures, *SIAM Journal of Scientific Computation* 28 (3) (2006) 901–928.
- [25] X. Wan, G.E. Karniadakis, Solving elliptic problems with non-gaussian spatially-dependent random coefficients, *Computer Methods in Applied Mechanics and Engineering* 198 (2009) 1985–1995.
- [26] D. Xiu, *Numerical Methods for Stochastic Computation*, Princeton University Press, Princeton, 2010.
- [27] D. Xiu, J.S. Hesthaven, High-order collocation methods for differential equations with random inputs, *SIAM Journal of Scientific Computing* 27 (3) (2005) 1118–1139.
- [28] X. Yang, M. Choi, G. Lin, G.E. Karniadakis, Adaptive ANOVA decomposition of stochastic incompressible and compressible flows, *Journal of Computational Physics* 231 (2012) 1587–1614.